HY5 regulates GLK and GNC transcription factors to orchestrate photomorphogenesis in *Arabidopsis thaliana*

Ting Zhang[1,2,5], Rui Zhang[1,5], Xi-Yu Zeng[1,2,5], Lu-Huan Ye[1], Shi-Long Tian[2], Yi-Jing Zhang[3], Wen-Bin Zhou[4], Xin-Guang Zhu[1], Peng Wang[1,*]

1 Laboratory of Photosynthesis and Environmental Biology, CAS Center for Excellence in Molecular Plant Sciences (CEMPS), Chinese Academy of Sciences, Shanghai 200032, China
2 University of Chinese Academy of Sciences, Shanghai 200032, China
3 State Key Laboratory of Genetic Engineering, Collaborative Innovation Center of Genetics and Development, Department of Biochemistry, Institute of Plant Biology, School of Life Sciences, Fudan University, Shanghai 200438, China
4 Institute of Crop Sciences, Chinese Academy of Agricultural Sciences, Beijing 100081, China
5 These authors contributed equally to this work

* Author for correspondence: wangpeng@cemps.ac.cn (P.W.)

T.Z. and P.W. designed the study. T.Z. and R.Z. performed most of the experiments. X.-Y.Z. worked on the transcriptional activation and protein interaction. L.-H.Y. worked on the ChIP-qPCR experiments. S.-L.T. analyzed the RNA-seq data. P.W., Y.-J.Z., W.-B.Z., and X.-G.Z. wrote and revised the manuscript.

Short title: GLK and GNC regulate photomorphogenesis

One-sentence summary: GLK and GNC act downstream of HY5, and cooperate with HY5 and DET1, to regulate both chloroplast development and hypocotyl elongation during the transition from skotomorphogenesis to photomorphogenesis.

Abstract

Light induced de-etiolation is an important aspect of seedling photomorphogenesis. GOLDEN2 LIKE (GLK) and GATA NITRATE-INDUCIBLE CARBON-METABOLISM-INVOLVED (GNC) are master transcriptional regulators involved in chloroplast development, but whether they participate in photomorphogenesis is largely unknown. Here we show that ELONGATED HYPOCOTYL5 (HY5) binds to *GLK* and *GNC* promoters and activates their expression. HY5 also interacts with GLK proteins. Chlorophyll content in the de-etiolating seedlings of the *hy5 glk2* and *hy5 gnc* double mutants was lower than that in the single mutants. It was further found that GLK inhibited hypocotyl elongation, whereas GNC promoted hypocotyl elongation, and that both could superimpose on the *hy5* phenotype. Correspondingly, GLK and GNC differentially regulate the expression of cell elongation genes. DE-ETIOLATED 1 (DET1) destabilises GLK proteins. The light-grown traits exhibited by etioplast of *det1* mutant were attenuated in *det1 glk2* double mutant, while similar to *det1* mutant, photosystem genes were up-regulated to different extent in etiolated seedlings overexpressing *GLK2* or *GNC*. Our study reveals that GLK and GNC act downstream of HY5 and likely cooperate with HY5 and DET1 to orchestrate multiple developmental traits during the light-induced skotomorphogenesis to photomorphogenesis transition.

Introduction

Light serves as an indispensable resource and the essential regulator for plant growth. In addition to photosynthesis, light also play roles in regulating seed germination, seedling de-etiolation, organ development, flowering and other important physiological processes (Jiao et al., 2007). After germination in darkness, seeds first grow into etiolated seedlings, displaying long hypocotyls with

hooked tops and closed cotyledons. These characteristics are called skotomorphogenesis. Once the etiolated seedlings break through the soil surface and receive light, hypocotyl elongation is inhibited, cotyledons open, chloroplasts develop, and photosynthesis begins. This series of processes is referred to as photomorphogenesis. Skotomorphogenesis and photomorphogenesis together ensure that etiolated seedlings emerge from the soil and develop into normal healthy seedlings, and are both a prerequisite for plant growth and development (Sullivan and Deng, 2003; Jiao et al., 2007).

As a positive regulator of photomorphogenesis, HY5 acts downstream of photoreceptors, such as cryptochromes, phytochromes and UV RESISTANCE LOCUS8 (UVR8), and plays important roles in seedling de-etiolation (Jiao et al., 2007; Stracke et al., 2010). Studies have shown that over 3000 genes can be directly regulated by the basic leucine zipper (bZIP) transcription factor HY5 (Jakoby et al., 2002; Lee et al., 2007; Zhang et al., 2011). It regulates many basic plant growth and development processes, including cell elongation, cell proliferation, chloroplast development, pigment accumulation, and nutrient uptake (Oyama et al., 1997; Shin et al., 2007; Jing et al., 2013). HY5 binds to promoters through G-box elements and inhibits the expression of cell elongation genes, such that *hy5* mutants show a typical long hypocotyl phenotype (Jing et al., 2013; Xu et al., 2016b). HY5 is important for chlorophyll and carotenoid accumulation under light as it regulates the expression of key enzymes such as PHYTOENE SYNTHASE (PSY) and PROTOCHLOROPHYLLIDE OXIDOREDUCTASE C (PORC). It also regulates the expression of photosynthetic pigment proteins, such as light-harvesting chlorophyll-protein complex I subunit A4 (LHCA4) (Toledo-Ortiz et al., 2014). HY5 functions through many different regulatory interactions. For example, it interacts with HY5-HOMOLOGY (HYH) or CALMODULIN7 (CAM7) protein to binds to the HY5 promoter and activate its own

expression (Kushwaha et al., 2008; Abbas et al., 2014; Binkert et al., 2014). The interaction between HY5 and B-box-containing (BBX) protein BBX21-BBX22 enhances the promoting effect of HY5 on photomorphogenesis, whereas the interaction between HY5 and BBX24-BBX25 does the opposite, suggesting that BBX protein acts as coregulator of HY5, for fine-tuning of photomorphogenesis (Datta et al., 2007; Datta et al., 2008; Xu et al., 2016a). Furthermore, HY5 interacts with PIF1 and PIF3 proteins to coordinate the production of reactive oxygen species and the temperature control of photosynthetic gene expression (Chen et al., 2013; Toledo-ortiz et al., 2014). In the case of excess HY5 protein, it can activate the expression of COP1, thus inducing the degradation of HY5 protein and maintaining it at a relatively stable level (Huang et al., 2012).

GOLDEN2 (G2)-LIKE (GLK) and GATA NITRATE-INDUCIBLE CARBON METABOLISM-INVOLVED (GNC) are two types of transcription factors directly involved in the regulation of chloroplast development. GLK transcription factors belong to the GARP superfamily (Fitter et al., 2002), which consists of GLK (initially from maize), Arabidopsis RESPONSE REGULATOR-B (ARR-B) and PHOSPHATE STARVATION RESPONSE 1 (PSR1) from Chlamydomonas (Hall et al., 1998; Imamura et al., 1999; Wykoff et al., 1999). GLKs were first found to regulate chloroplast development in maize, with a pair of GLK homologs ZmG2 and ZmGLK1 expressed in bundle sheath and mesophyll cells respectively (Hall et al., 1998; Rossini et al., 2001). In Arabidopsis, GLK1 and GLK2 are regulated by light, and function redundantly in regulating chlorophyll biosynthesis and chloroplast development. The leaves and siliques of the double mutant are pale green, and thylakoid development in the chloroplasts is retarded (Fitter et al., 2002). Overexpression of GLK1 or GLK2 in *glk1 glk2* double mutants can restore the defect in chloroplast development (Waters et al., 2008). Ectopic expression of GLKs was also able to induce increased chloroplast numbers in non-green

tissues such as roots and callus of Arabidopsis and rice (Nakamura et al., 2009; Kobayashi et al., 2012a), and in tomato fruits (Nguyen et al., 2014). GLK target genes are mainly related to chlorophyll biosynthesis, light-harvesting, and electron transport (Waters et al., 2009; Kobayashi et al., 2012b). In the process of seedling de-etiolation, GLKs interact with and are phosphorylated by BRASSINOSTEROID INSENSITIVE2 (BIN2) protein, which promotes the stability and transcriptional activity of GLK1 (Zhang et al., 2021). GLK also interacts with ORESARA 1 (ORE1) protein during senescence, with ORE1 antagonizing GLK induction of target genes (Rauf et al., 2013). The degradation of GLK protein itself is related to ubiquitination, with GLK2 shown to interact with DET1 protein in tomato prior to processing by CUL4-DDB1 ubiquitin E3 ligase for degradation (Tang et al., 2016).

The *GATA NITRATE-INDUCIBLE CARBON-METABOLISM-INVOLVED* (*GNC*) gene was identified by screening mutants on nitrogen-deficient medium, with *gnc* mutants accumulating lower chlorophyll than wild type (Bi et al., 2005). The *CYTOKININ-RESPONSIVE GATA FACTOR1* (*CGA1*) gene is strongly induced by cytokinin, and CGA1 is involved in the cytokinin signaling (Naito et al., 2007). The *gnc cga1* double mutant exhibits decreased chlorophyll content and decreased chloroplast number. Overexpression of *GNC* or *CGA1* in Arabidopsis resulted in obvious chloroplast development in seedling roots and hypocotyls, and increased chloroplast number in cotyledon and leaf epidermal cells (Chiang et al., 2012). Overexpression of *CGA1* in rice increases chloroplast number as well as starch biosynthesis in the leaves (Hudson et al., 2013; Lee et al., 2021). In spite of the well-known downstream targets of GLK and GNC, their upstream regulation, particularly in the context of light signaling is not clear. As HY5 is a regulatory hub in light signaling, and it has been reported that GLK and GNC are dependent on HY5 in regulating root greening (Kobayashi et al., 2012a, 2017), the molecular

relationships between HY5, GLK, and GNC during seedling development are in need of systematic analysis. It is also important to consider the role of the COP/DET/FUS complex in regulating GLK and GNC stabilities. DET1 is involved in the ubiquitination and degradation of positive regulators of photomorphogenesis in darkness. Apart from shorter hypocotyls and opened cotyledons, the dark-germinated *det1* mutant seedlings show part of the light-grown traits, such as expression of photosynthetic genes and development of thylakoid membranes (Chory et al., 1989). The molecular mechanism behind such phenotypes in the dark is not fully understood and the potential involvement of GLK or GNC is worth considering.

Therefore, this study focused on the molecular and functional linkages among HY5, GLK, and GNC/CGA1 transcription factors, aiming to analyze and clarify the local regulatory network connecting them, so as to better understand the relationships between light signaling, seedling formation, and chloroplast development during photomorphogenesis. At the same time, relationships between GLK, GNC, and DET1, and their effects on the expression of photosynthetic genes in etiolated seedlings were examined. The results shed light on the concerted involvement of HY5, GLK, and GNC/CGA1 transcription factors in both skotomorphogenesis and photomorphogenesis.

Results

HY5, GLK1/2, and GNC/CGA1 regulate chlorophyll content to different extents in de-etiolating Arabidopsis seedlings

HY5, GLKs, and GNC/CGA1 have been reported to regulate the expression of chlorophyll biosynthesis and photosynthesis related genes (Fitter et al., 2002; Lee et al., 2007; Waters et al., 2009; Chiang et al., 2012; Hudson et al., 2013; Toledo-ortiz et al., 2014). To explore the significance of these regulations during

photomorphogenesis, we performed systematic investigation in de-etiolating seedlings. All plants were grown in darkness for 4 days, and then sampled at different time points in white light to determine chlorophyll content. It was found that the chlorophyll content in *glk1* mutant had no or little difference from the wild type, while it was significantly lower in *glk2* mutant, and it decreased more significantly in *glk1 glk2* double mutant **(Figures 1A and 1C; Supplemental Figures S1A and S1C)**. This indicates that both GLKs affect chlorophyll biosynthesis in seedling de-etiolation process and GLK2 may play a dominant role. Overexpression of GLK1 or GLK2 in double mutants can compensate for the phenotype of decreased chlorophyll **(Supplemental Figures S1A and S1C)**. The chlorophyll content of *cga1* mutants was not notably different from the wild type, while it was lower in *gnc* and *gnc cga1* double mutants, but the difference was much smaller than that between *glk2* related mutants and the wild type **(Figures 1B and 1D; Supplemental Figures S1B and S1D)**. The chlorophyll content of *35S:GNC* overexpressed material was significantly higher than that of the wild type in the greening process, while it showed no difference in *35S:CGA1* overexpressed material from that of the wild type at this stage **(Supplemental Figures S1B and S1D)**. The chlorophyll content of *hy5* mutant was lower than that of the wild type, and overexpression of HY5 in the mutant could effectively compensate for the phenotype **(Figure 1; Supplemental Figure S1)**. We checked the expression of *GLK1*, *GLK2*, *GNC*, and *CGA1* genes in the de-etiolation process of wild type seedlings, and found that the expression levels of *GLK2* and *GNC* were more prominent in response to light **(Figure 1E)**, demonstrating again the relative greater importance of them to seedling greening.

Loss of *GLK1/2* or *GNC/CGA1* function combined with *HY5* mutation has limited further effects on seedling greening

In order to elucidate the genetic relationships between HY5, GLKs and GNC/CGA1, we constructed double and triple mutants, and investigated the chlorophyll content in seedlings during de-etiolation. It was found that the chlorophyll content of *hy5 glk1* double mutant was not different from that of the wild type and *glk1*. We noticed that the *glk1* single mutant used was caused by an insertion in the promoter region, and thus the phenotypes in *glk1* single mutant and *hy5 glk1* double mutant may not be representative of null alleles. On the other hand, the chlorophyll content of *hy5 glk2* double mutant was lower than that of *glk2* or *hy5* mutant at 12 h during greening. However, there was no difference in chlorophyll content between *hy5 glk1 glk2* triple mutant and *glk1 glk2* double mutant during de-etiolation **(Figures 1A and 1C)**. The chlorophyll content in *hy5 gnc* and *hy5 cga1* mutants showed little or no difference compared to *hy5*, and only *hy5 gnc cga1* triple mutant exhibited notably lower chlorophyll content at 12 h during greening. Moreover, the chlorophyll content of these mutants was generally higher than that of the *glk* related double or triple mutants **(Figures 1B and 1D)**.

In order to clarify the chlorophyll phenotype of *hy5* and *glk2* mutants, we verified the expression levels of some chlorophyll biosynthesis and photosystem genes in de-etiolating seedlings. At 12 h of light exposure, the expression levels of chlorophyll biosynthesis genes (*HEMA1*, *PORB*, *PORC* and *CAO*) in *hy5*, *glk2* and *hy5 glk2* mutants were all remarkably lower than those in the wild type. The decrease in *glk2* and *hy5 glk2* mutants was not lower than that in the *hy5* mutant, except for *PORB* **(Figure 2A)**. The expression levels of photosystem light harvesting genes (*LHCB1.2*, *LHCB2.2*, *LHCA1* and *LHCA4*) was also significantly lower in *hy5*, *glk2*, and *hy5 glk2* mutants than in the wild type, with their expression in *hy5* mutant considerably higher than those in *glk2* and *hy5 glk2* mutants **(Figure 2B)**. These results indicate that during de-etiolation of seedlings GLK2 has stronger regulation on photosystem light harvesting genes than HY5,

whereas their regulation on chlorophyll biosynthesis may be comparable.

To further complement the observed phenotype, we moved on to analyse the seedlings grown under continuous white light for 4 days, and found similar differences of chlorophyll content to that during de-etiolation. However, the chlorophyll content in *hy5 glk1 glk2* triple mutant was lower than that in *glk1 glk2* double mutant **(Figures 2C and 2D)**. We investigated the chloroplast development in wild type, *glk1 glk2*, *hy5*, and *hy5 glk1 glk2* mutants under continuous light exposure. Transmission electron microscopy showed that the chloroplast size of *glk1 glk2* and *hy5 glk1 glk2* mutants was smaller than that of the wild type and *hy5* mutant, the accumulation of starch grains was decreased, and the thylakoid stacking was sparser. Even worse, *hy5 glk1 glk2* triple mutant showed obvious fractured stromal thylakoids **(Figure 2E)**, suggesting that *HY5* mutation combined with *GLK1* and *GLK2* double mutations can lead to further defects in chloroplast development.

HY5 directly regulates *GLK1*, *GLK2*, *GNC* and *CGA1* gene expression

As an extension of the results shown in **Figure 1E**, we found that the expression levels of *GLK1*, *GLK2*, *GNC* and *CGA1* genes in *hy5* mutants were significantly lower than those in the wild type **(Figures 1F)**, indicating that HY5 positively regulates their expression. Typical *cis*-elements to which HY5 binds to regulate target gene expression include G-box (CACGTG), T/G-box (CACGTT), E-box (CAATTG), ACE-Box (ACGT), and Z-Box (ATACGGT) (Shin et al., 2007; Chang et al., 2008; Catala et al., 2011; Abbas et al., 2014). We performed promoter analysis for *GLK1* and *GLK2*, and found that their promoter regions contained HY5-binding *cis*-elements. These regions were synthesized to conduct electrophoretic mobility shift assays (EMSA). It was shown that HY5 could bind to *GLK1* and *GLK2* promoter sequences, competitive probes weakened such

binding, while the binding ability of mutant probes was much lower than that of normal probes **(Figure 3A)**. In parallel, by transforming protoplasts dual-luciferase assay displayed that HY5 could activate *GLK1* and *GLK2* expression **(Figures 3B and 3C)**. While obtaining the above *in vitro* results, we also validated the binding *in vivo* via chromatin immunoprecipitation (ChIP) coupled with quantitative PCR (qPCR) assay. Three or two regions containing HY5 binding elements were selected from the promoters of *GLK1* and *GLK2* respectively, and the results demonstrated that the P2 region from *GLK1* promoter and the P1 region from *GLK2* promoter were most strongly bound by HY5 **(Figure 3D)**. *In vitro* experiment EMSA and dual-luciferase assays confirmed that HY5 could also bind to *GNC* and *CGA1* promoters to activate their transcription, again followed by *in vivo* experiment ChIP-qPCR showing that the highest enrichment of P1 on *GNC* and *CGA1* promoters by HY5 **(Figure 3)**. In conclusion, HY5 directly binds to the promoters of *GLK1*, *GLK2*, *GNC*, and *CGA1* to activate their gene expression.

GLK1/2 and GNC/CGA1 oppositely regulate hypocotyl elongation of light-grown seedlings

HY5 is known to inhibit hypocotyl elongation during photomorphogenesis, as *hy5* seedlings exhibit longer hypocotyls (Sullivan and Deng, 2003; Jiao et al., 2007). Since we found that HY5 directly regulates the expression of *GLK*, *GNC*, and *CGA1* genes, whether GLK, GNC and CGA1 also play roles in seedling morphological development upon light regulation became the next question. Therefore, we systematically investigated the hypocotyl phenotypes of a series of *glk*, *gnc*, and *cga1* mutants. The hypocotyl length of *glk* mutants was measured under different light quality, and those in *glk1*, *glk2* and *glk1 glk2* mutants were longer than in wild type, while shorter than in *hy5* mutant, after germinating and growing under white, blue or red light for 4 days **(Figures 4A and 4B)**. When

GLK1 or *GLK2* were overexpressed in *glk1 glk2* mutants, the hypocotyl length was restored to the level of wild type. There was no significant difference in hypocotyl length between the mutants and wild type after germinating and growing for 4 days in darkness **(Supplemental Figure S3)**. Together the above results indicate that GLK inhibits hypocotyl elongation during light-induced seedling development.

We further investigated the hypocotyl phenotype in *hy5* and *glk* double and triple mutants. Under white or blue light, compared with *hy5*, hypocotyls of *hy5 glk1* were slightly longer, while hypocotyls of *hy5 glk2* and *hy5 glk1 glk2* were significantly longer than that of *hy5*. The hypocotyls of all materials were generally longer under red light, and those of *hy5 glk1*, *hy5 glk2* and *hy5 glk1 glk2* were still longer than those of *hy5*, but with smaller differences. No notable differences in hypocotyl length were observed in dark-grown seedlings between wild type and these mutants **(Figures 4A and 4B)**. We measured the cell length of wild type, *glk1 glk2*, *hy5*, and *hy5 glk1 glk2* materials in the middle segment of hypocotyls growing under white light for 4 days, and found that the hypocotyl cell length of *glk1 glk2* mutant was longer than that of the wild type, and that of *hy5 glk1 glk2* mutant was longer than that of *hy5* mutant **(Figures 4C and 4D)**. In general, there is an obvious trend of *hy5* < *hy5 glk1* < *hy5 glk2* < *hy5 glk1 glk2* in hypocotyl length, and GLKs may work independent (at least partly) of HY5 to inhibit hypocotyl elongation, with GLK2 playing a more important role than GLK1.

Different from the hypocotyl phenotype of *glk* series mutants, after germinating and growing under white light for 4 days, the hypocotyl length of *gnc*, *cga1* and *gnc cga1* mutants was shorter than that of the wild type, while the hypocotyl length of *35S:GNC* and *35S:CGA1* overexpressed materials was longer than that of the wild type. There was no difference in hypocotyl length between these mutants and wild type after germinating and growing in darkness

(Supplemental Figure S4), indicating that GNC and CGA1 promoted hypocotyl elongation under white light. In addition, the hypocotyl length of *hy5 gnc*, *hy5 cga1* and *hy5 gnc cga1* mutants was shorter than that of *hy5* under white light, but significantly longer than that of *gnc*, *cga1* and *gnc cga1* mutants **(Figures 4E and 4F)**, indicating that GNC and CGA1 were able to reduce the inhibition of HY5 on hypocotyl elongation.

Transcriptome and RT-qPCR analysis reveals differential regulation of cell elongation genes by HY5, GLK2, and GNC

The above results showed that the phenotype of *hy5 glk2* mutant was more severe than that of the *hy5 glk1* mutant, both in regulating chlorophyll content and inhibiting hypocotyl elongation. Hence, we selected wild type, *glk2*, *hy5*, and *hy5 glk2* seedlings that germinated and grew for 4 days under white light for transcriptome sequencing. As shown in a Venn diagram, *glk2*, *hy5*, and *hy5 glk2* mutants jointly affected the expression of 142 genes, including 138 down-regulated genes and only 2 up-regulated genes **(Figure 5A)**. Deletion of *HY5* or *GLK2* in most cases resulted in down-regulation of genes, and K-means clustering showed the same trend **(Figure 5B)**, in line with the expectation of them as positive regulators of photomorphogenesis. Most up-regulated genes were expressed in *hy5* and *hy5 glk2* mutants. Among the down-regulated genes, 385 were down-regulated together in *hy5* and *hy5 glk2* mutants, while 201 were down-regulated together in *glk2* and *hy5 glk2* mutants. This is consistent with HY5's upstream position in activating *GLK* gene expression mentioned above. The remaining 91 down-regulated genes only in *hy5 glk2* mutants may represent targets of combined HY5 and GLK activity **(Figure 5A)**. According to the trend of *glk2* < *hy5* < *hy5 glk2* in hypocotyl length, K4 and K7 groups from K-means clustering could be considered for investigating GLK2 and HY5 regulated

hypocotyl elongation **(Figure 5B)**. In addition, heat map was generated from differential expression of a list of known cell elongation genes, and a series of up-regulated genes were considered for subsequent validation **(Figure 5C)**.

Several elongation genes from **Figure 5C** were selected for RT-qPCR verification. Among the expression levels of *EXPA5*, *IAA19*, *SAUR20*, and *PME16*, most of them expressed higher in *glk2* than in wild type, and higher in *hy5* than in *glk2*. They were detected higher in *hy5 glk2* than in *hy5*, with more variable degrees **(Figure 5D)**. We hypothesized that the interaction between GLK2 and HY5 proteins could enhance the inhibitory effect on these elongation genes, and GLK2 may independently inhibit some elongation genes. We also analysed the expression levels of selected elongation genes in *gnc* and *hy5 gnc* materials. The expression level of *IAA7* in *gnc* mutant was lower than that in wild type, and the expression levels of several other genes in *gnc* mutant tended to be lower than in wild type, although not significant **(Figure 5E)**. In addition, the expression levels of *IAA7*, *IAA19*, *XTH4*, and *PME16* appeared lower in the *hy5 gnc* double mutant than in *hy5* mutant **(Figure 5E)**. These results indicate that GNC could promote the expression of these elongation genes to less and varying degrees, both independently or on top of HY5. The primarily targeted hypocotyl elongation genes by GNC/CGA1 may be largely different from those by GLKs.

Interaction of HY5 and GLK proteins

Apart from directly targeting many genes to promote their expression, HY5 also interacts with other proteins, HYH or HFR1 for instance, to mutually enhance protein stability, or together bind to *HY5* or downstream gene promoters (Lee et al., 2007; Ciolfi et al., 2013; Jang et al., 2013). The interaction between HY5 and G-box binding factor 1 (GBF1) attenuates the activation of *RBCS-1A* by HY5. Since HY5 interacts with GBF1, and GBF1 interacts with GLK (Tamai et al., 2002;

Singh et al., 2012; Ram et al., 2014), we then examined the possibility of HY5 interacting with GLK proteins. In pull-down experiments, the experimental group GST-GLK1 and GST-GLK2 could pull down HY5 protein, while the control group could not **(Figure 6A)**, indicating that HY5 binds to GLK1 and GLK2. Through bimolecular luminescence complementation assays, it was found that luciferase signal could be detected when HY5 was co-transfected with GLK1 and GLK2 proteins, while the signal was not present in the negative controls **(Figure 6B)**, indicating that HY5 interacts with GLK1 and GLK2. The above experiments provide *in vitro* evidence of HY5 and GLK interaction. We then performed co-immunoprecipitation assays to confirm that GLK2 interacts with HY5 *in vivo*. GLK2 fusion protein was immunoprecipitated with FLAG beads, then HY5 fusion protein was co-precipitated, and was detected by anti-GFP antibody **(Figure 6C)**. HY5 might first activate the expression of *GLK*, and then interacts with GLK protein to regulate common targets. It should be also pointed out that extra factors might exist to coordinate the effects of HY5 and GLK2 on their target genes.

GLK2 content affects the plastid ultrastructure and photosystem gene expression in dark-grown *det1* mutant of Arabidopsis

Compared to the traits of photomorphogenesis, the morphology and gene expression changes of skotomorphogenesis are relatively less addressed by previous researches. One of the few but well known observations is that, the stromal thylakoid membrane was found sufficiently extended in the plastids of etiolated *det1* mutant seedlings rather than the default form of prolamella body, and some photosynthetic genes were already expressed in the dark (Chory et al., 1989). On account of the emphasis on GLK2 from above, we constructed *det1 glk2* double mutant and comparative observations were made on the plastid ultrastructure in the cotyledons of dark-grown *det1*, *glk2*, and *det1 glk2* mutants.

As expected, the cotyledons were open in the etiolated *det1 glk2* mutant, and paler in the light-grown *det1 glk2* mutant **(Figure 7A)**. We found that the thylakoid lamellae in the plastids of *det1 glk2* mutant were less developed than in *det1* mutant in the dark, although in both cases there was little evidence of a prolamellar body, indicating that the developed chloroplasts in etiolated *det1* mutant were related to GLK2 function. By contrast, there was no significant structural difference of the prolamellar body in *glk2* mutant and *GLK2*-overexpressing line compared with the wild type, but the size was smaller or larger respectively **(Figure 7B)**.

It is known that in the dark, HY5 ubiquitination and degradation are mediated by the COP/DET/FUS complex (Saijo et al., 2003). In order to study the stability of GLK proteins in Arabidopsis, we examined the dark-grown wild type and *det1* mutant using Arabidopsis GLK1 and GLK2 antibodies for Western-blots. The results showed that both GLK1 and GLK2 protein contents in *det1* mutant were higher than those in the wild type **(Figure 8A)**, suggesting that DET1 may promote the degradation of GLK proteins. It should be noted that Rubisco large subunit (RbcL) content was higher in *det1* than in the wild type, which is consistent with the increased accumulation of *RbcL* transcript in dark-grown *det1* mutant (Chory et al., 1989). After MG132 (a proteasome inhibitor) treatment, the accumulation of GLK proteins in the wild type was higher than that in the DMSO control group, but still much lower than that in the *det1* mutant **(Figure 8A)**. The deficiency of DET1 likely blocked the upstream steps of protein degradation such as ubiquitination, so that the significant accumulation of GLK proteins in *det1* mutant was less affected by MG132. Supportively, *in vitro* protein binding experiments indicate that DET1 interacts with both GLK1 and GLK2 proteins **(Supplemental Figure S8A)**, and GNC and CGA1 proteins as well **(Supplemental Figure S8B)**.

The expression of photosynthetic genes in dark-grown *det1* mutant seedlings is interesting (Chory et al., 1989), but the mechanism of these genes being turned off in skotomorphogenesis, has not been elucidated. We measured the expression of photosystem genes in a group of dark-grown *det1* and *glk2* related mutants, and found that the expression levels of *LHCB1.2* and *LHCA1* were much higher in *det1* mutant, but were lower in *glk2* mutant than those in wild type. The down-regulation of these genes by GLK2 was also found in *det1 glk2* double mutant comparing with the *det1* mutant **(Figure 8B)**. This indicates that GLK2 contributes significantly to the expression of photosystem genes in dark-grown seedlings, and the effects could be additive to the loss of DET1 function. In the etiolated materials overexpressing *GLK1*, *GLK2*, *GNC* or *CGA1*, the expression of *LHCB1.2* and *LHCA1* genes were significantly promoted in *GLK1* or *GLK2* overexpression lines, less promoted in the *GNC* overexpression line, and least changed in the *CGA1* overexpression line **(Figure 8C)**. When grown this same set of materials in the light, increased expression of *LHCB1.2* and *LHCA1* genes were still observed to larger extent in *GLK1* or *GLK2* overexpression lines than in *GNC* and *CGA1* overexpression lines relative to the wild type **(Figure 8D)**. Notably, expression levels of *LHCB1.2* and *LHCA1* genes also increased in both dark and light-grown *HY5* overexpression lines, but were not higher than those in *GLK1* or *GLK2* overexpression lines, indicating again that GLKs function at least partly independent of HY5 during seedling photomorphogenesis.

Discussion

In this work, we have constructed a series of mutant materials to systematically study the regulatory relationships between HY5, GLK, and GNC/CGA1 transcription factors, as well as their stabilities and functions within the scenario of skotomorphogenesis and photomorphogenesis. We find that: (1) HY5 directly

activates *GLK*, *GNC*, and *CGA1* expression, and together they positively regulate chlorophyll biosynthesis and photosystem formation; (2) GLK proteins inhibit hypocotyl elongation, whereas GNC and CGA1 promote hypocotyl elongation, by differentially regulating the expression of cell elongation genes; (3) In the dark, DET1 destabilises GLK proteins, and the abnormal light-grown traits exhibited in the etioplast of *det1* mutant seedlings can be attributed to GLK2 activity; (4) GLK2 maybe the predominant regulator of photosynthetic genes, during both skotomorphogenesis and photomorphogenesis. At present, the molecular mechanism of GLK and GNC in regulating hypocotyl elongation is not entirely clear. These need to be further investigated in combination with specific genetic material construction. In addition, GLK2 function has been standing out in multiple ways, partially recruited by and interact with HY5, and effectively compensates for HY5 function, so that it deserves targeted studies in order to guide the potential application of GLK2 and HY5 in crop enhancement.

GLK and GNC function downstream but partially independent of HY5 in seedling greening

HY5 and GLK both functions in regulating chlorophyll biosynthesis and chloroplast development, but targeted studies and clear conclusions are missing on whether or how the two are related. Studies have shown that PHYTOCHROME-INTERACTING FACTOR 4 (PIF4) in Arabidopsis binds to the promoters of *GLK1* and *GLK2* to inhibit their expression (Song et al., 2014), while HY5 antagonises PIFs to regulate the biosynthesis of photosynthetic pigments (Tolede-Ortiz et al., 2014). Besides, microarray studies showed that both phytochrome A and phytochrome B regulate GLK transcription (Tepperman et al., 2006). Considering that HY5 acts downstream of the photoreceptors, and is a high-level regulator (many HY5 targets are other transcription factors) of

469 photomorphogenesis (Lee et al., 2007), there may be a direct positive regulation
470 of HY5 to *GLKs*. We provided experimental evidences in this work that HY5
471 indeed binds to the promoters of *GLK* genes and activates their expression.
472 Similarly, the HY5 regulation of *GNC* and *CGA1* was also confirmed **(Figure 3)**.

473 We have constructed double and triple mutants of HY5, GLK1/2, and
474 GNC/CGA1 to study their functional relationships. Only limited decrease of
475 chlorophyll content and related gene expression were observed when *hy5 glk2*
476 mutant was compared to *glk2* mutant, or *hy5 glk1 glk2* mutant was compared to
477 *glk1 glk2* mutant **(Figures 1 and 2)**. Our transcriptome data indicate that,
478 compared with HY5, GLK2 tends to positively affect more PSII and PSI related
479 genes **(Supplemental Figure S7)**, which was also supported by the stronger
480 regulation of GLK2 on light harvesting genes than HY5 **(Figure 2B)**. When
481 overexpressing *GLK2* in the *hy5* mutant, the chlorophyll level increased
482 significantly, although it was still lower than overexpressing *GLK2* in wild type (Liu
483 et al., 2021). Our study clarifies the downstream relationship of GLKs to HY5, and
484 implies that GLKs contributes more intensively than HY5, to Arabidopsis seedling
485 greening.

486 It has been reported that HY5 and GLK2 are involved in the greening of
487 detached root in Arabidopsis, and that the GLK2 regulation of root greening
488 depends to some extent on the presence of HY5 (Kobayashi et al., 2012a). We
489 observed that the detached roots could still turn green in the absence of a single
490 GLK or both GLKs, but not in the absence of HY5 **(Supplemental Figure S5)**.
491 The greening process is promoted by the accumulation of endogenous cytokinin
492 in detached roots (Kobayashi et al., 2012a). In order to investigate the effect of
493 HY5 and GLKs on cytokinin regulated leaf greening, we added
494 6-Benzylaminopurine (6-BA) during seedling greening of *hy5 glk* series mutants.
495 Results showed that 6-BA treatment could promote the accumulation of

chlorophyll during this process, with or without GLKs or HY5 **(Supplemental Figure S6)**. These results suggest that GLKs and HY5 play similar roles in response to cytokinin to promote chlorophyll biosynthesis in leaves, whereas HY5 plays a more significant role in detached roots.

GLKs seem to exert stronger regulation than GNC/CGA1 in seedling greening, as *glk* series mutants are much paler than *gnc/cga1* series mutants **(Figure 1; Supplemental Figure S1)**. No difference in chlorophyll content between *glk1 glk2 gnc cga1* quadruple mutant and *glk1 glk2* mutant was found, and *CGA1* overexpression in *glk1 glk2* mutant could not restore the chlorophyll content, while overexpression of *GLK1* partially restores the chlorophyll content in *gnc cga1* mutants (Bastakis et al., 2018). Zubo et al. suggested that GLK1/GLK2 and GNC/CGA1 play both overlapping and independent roles in regulating chlorophyll biosynthesis and chloroplast development (Zubo et al., 2018). We further propose that GLKs may play more prominent roles than GNC/CGA1, downstream but partly independent of HY5, to regulate various targets during the de-etiolation process of photomorphogenesis.

Differential participation of GLK and GNC in HY5 regulated hypocotyl elongation

The inhibition of hypocotyl elongation, opening of cotyledon, and chloroplast development are continuous and inseparable processes during seedling photomorphogenesis. Since HY5 inhibits hypocotyl elongation, we were also curious about the potential GLK and GNC regulation of hypocotyls. It has been mentioned that *glk1* seedlings displayed longer hypocotyls and less separated cotyledons (Martín et al., 2016, Alem et al., 2022). By systematically analysing the hypocotyl phenotype of mutants and overexpression lines, we certified that both GLK1 and GLK2 inhibit hypocotyl elongation, with additive effects on the function

of HY5 **(Figures 4A and 4B; Supplemental Figure S3)**. Transcriptomic sequencing and RT-qPCR verification showed that GLK2 itself could inhibit the expression of elongation genes, and different elongation genes exhibited different regulatory responses to GLK2 and HY5 **(Figure 5E)**.

We noticed that the expression levels of some elongation genes were reported lower in *gnc cga1* mutants than in the wild type (Xu et al., 2017), and the seedlings of the *quintuple* mutant of *GNC*, *GNL*, and *B-GATA* had shorter hypocotyl than wild type (Ranftl et al., 2016). In this work, we have confirmed that, contrary to GLK's inhibitory effect, GNC and CGA1 promote hypocotyl elongation, and the mutation of GNC or CGA1 negatively affects the inhibition of hypocotyl lengths by HY5 **(Figures 4E and 4F; Supplemental Figure S4)**. Our results indicate that GNC could promote the expression of elongation genes to varying degrees, independently or on top of HY5 **(Figure 5E)**. It should be pointed out that the same elongation gene maybe differentially regulated by HY5, GLKs, or GNC/CGA1. In addition, the changes of elongation genes in *glk1 glk2*, *gnc cga1*, *hy5 glk1 glk2*, and *hy5 gnc cga1* mutants are worth exploring, to clarify the potential redundant or additive effect of them on hypocotyl length.

Significance of GLK2 and GNC in the context of skotomorphogenesis to photomorphogenesis transition

Traits of photomorphogenesis are negatively regulated by the COP/DET/FUS complex in the dark, which mediates the ubiquitination and proteasome degradation of positive regulators such as HY5, HYH, LAF1, and HFR1 (Osterlund et al., 2000; Holm et al., 2002; Seo et al., 2003; Yang et al., 2005). Interestingly, *det1* and *cop1* mutants exhibit some of the characteristics of photomorphogenesis during skotomorphogenesis, with shorter hypocotyls, open cotyledons, and expression of photosynthetic genes (Chory et al., 1989; Deng et

al., 1992). These phenotypes should be related to the accumulation of positive regulators of photomorphogenesis in darkness, but the specific regulators and their influence on the phenotypes are not clear. It has been reported that long-term ABA treatment activates the activity of COP1, which then interacts with GLK1 protein to mediate its ubiquitination and degradation (Tokumaru et al., 2017; Lee et al., 2021). In this study we further showed that DET1 is responsible for the protein degradation of both GLK1 and GLK2 in Arabidopsis seedlings **(Figure 8A)**. As for GLK2, we have constructed *det1 glk2* mutant in Arabidopsis to compare with *det1* mutant during skotomorphogenesis. The overall number of extended thylakoid lamellae and expression of photosystem genes were found markedly reduced in *det1 glk2* compared with *det1* mutant **(Figures 7B and 8B)**. In fact, both GLK2 and GLK1 contribute significantly to the expression of photosystem genes, not only in the light but also in dark-grown seedlings, while GNC and CGA1 seem to contribute less than GLKs **(Figures 8C and 8D)**. Thus, the appropriate function of GLKs and GNC/CGA1 is regulated at protein level by DET1 in etiolated seedlings, while upon light HY5 takes the transcriptional control and at least partly coordinates their functions, in a regulation cascade of light, HY5, and GLKs or GNC/CGA1.

We constructed a working model as shown in **Figure 9**. In dark-grown seedlings, GLKs, GNC, CGA1 and HY5 proteins are subjected to the DET1 mediated degradation. Photosynthetic genes are inactive and plastid inner membranes stay at prolamellar body status. After exposure to light, DET1 activity is inhibited and GLK, GNC, CGA1 and HY5 proteins accumulate. HY5 activates *GLK*, *GNC* and *CGA1* genes in a light-dependent manner, and likely interact with their proteins to cooperatively regulate downstream gene expression to promote photomorphogenesis. GLKs are master regulators of chloroplast development

and able to inhibit hypocotyl elongation independent of HY5. GNC and CGA1 are less dominant in chloroplast development and able to promote hypocotyl elongation. These could be the compensation for the relatively weak regulation of HY5 on chloroplast development, and a sensible way to orchestrate light induced seedling development, by recruiting multitasking yet complementary regulators. Our study systematically reveals the new function of GLK and GNC regulating hypocotyl length under light, refines the local network of HY5, GLKs, GNC and CGA1, and provides new perspective for better understanding the transition between dark and light-grown seedlings.

Materials and methods

Plant materials and growth conditions

Arabidopsis mutants used in this study were in the Columbia (Col-0) background. The *glk1*, *glk2*, *glk1 glk2*, *gnc*, *cga1*, *gnc cga1*, *hy5*, and *det1* mutants (Chory et al., 1989; Oyama et al., 1997; Fitter et al., 2002; Chiang et al., 2012), as well as *35S:GLK1 glk1 glk2*, *35S:GLK2 glk1 glk2*, *35S:GNC*, and *35S:CGA1* overexpression plants (Waters et al., 2008; Chiang et al., 2012) were described previously. Other mutants described in this study were created by crossing from the above materials. Surface-sterilized seeds were sown onto half-strength Murashige and Skoog (MS) medium, which contained 1% sucrose and 0.8% agar, and were cold-treated at 4°C in darkness for 3 days to ensure synchronized germination, followed by growing in dark or light chambers maintained at 22°C.

Chlorophyll measurements

Total chlorophylls were extracted by homogenizing the seedlings in 80% acetone, and leaving the solutions at 4°C for overnight incubation. The absorbance was detected at wavelength OD_{652} with a spectrophotometer. Chlorophyll

concentration Ca+b was calculated by OD_{652}/34.5 (mg/mL), and then converted according to the fresh weight of the material (Arnon, 1949; Zhao et al., 2016).

Hypocotyl length measurement

To measure the hypocotyl length of seedlings, seeds were sown on plates and stratified at 4°C in darkness for 3 d, and then kept in white light for 4 h in order to induce uniform germination. The seeds were then transferred to white, blue, red light, or dark conditions and incubated at 22°C for 4 d. The hypocotyl length were measured using ImageJ software after photographing the seedlings.

Transmission electron microscopy

Leaf sections of 2 mm size were cut from the seedlings and fixed in 2.5% glutaraldehyde, with low vacuum applied for 60 min to assist fixation. Post fixation in osmium tetroxide, embedding in Spurr's resin, and other steps were performed by the TEM platform in Center for Excellence in Molecular Plant Sciences, following standard procedures. The ultra-thin sections were imaged at 80 KV with a Hitachi H-7650 transmission electron microscope.

Quantitative RT-PCR

Total RNA was extracted from Col-0 and mutant seedlings using an RNAiso Plus kit (Takara). Complementary DNAs (cDNA) were synthesized from 2 μg of total RNA using a Prime Script RT Reagent Kit, with a genomic DNA Eraser (Yeasen). Then, cDNA was subjected to RT-qPCR assays, using the Step One Plus RT-PCR detection system (Applied Biosystems) and SYBR Green PCR Master Mix (Yeasen). PCR was performed in triplicate for each sample, and the expression levels were normalized to that of *ACT7* gene.

Immunoblot analysis

Seedlings were homogenized in a protein extraction buffer containing 100 mM Tris (pH 6.8), 10% Glycerol, 0.5% SDS, 0.1% Triton, 5 mM EDTA, 0.01 M DTT, and 1 × complete protease inhibitor cocktail (Roche). Equal amount of proteins were loaded and separated on a 10% SDS-PAGE gel and transferred to polyvinylidene fluoride membrane. The membrane was blocked with 5% milk and incubated with primary antibody overnight at 4°C, washed four times with 1 × Phosphate Buffered Saline Tween-20 (PBST) for 5 minutes, and incubated with secondary antibody for 1 h at room temperature. After four washes with PBST for 5 minutes, signal was detected with ECL kit (Millipore).

EMSA assay

Synthetic complementary oligonucleotides of *GLK1*, *GLK2*, *GNC*, and *CGA1* (or mutant probe with HY5 binding motif mutation) were obtained, and probes were PCR amplified using Cy5-labeled primers. For proteins, the coding sequence of HY5 was cloned into pCold-TF vector, expressed, and purified with Capturem™ His-Tagged Purification Maxiprep Kit (Takara). The binding reaction was performed in 20 μL binding buffer (10 mM Tris pH 8.0, 1 mM KCl, 4 mM $MgCl_2$, 0.5mM DTT, 5% glycerol, 0.2 mM EDTA, and 0.01% BSA) using 15 nM probes and 200 ng proteins, and incubated at room temperature for 30 min. The reactions were resolved by electrophoresis in a 6% (v/v) native polyacrylamide gel at 4°C. Cy5-labeled DNA in the gel was scanned by an Amersham Typhoon 5 Biomolecular Imager.

Dual-luciferase reporter system

Promoter sub-fragments of *GLK1*, *GLK2*, *GNC*, and *CGA1* were cloned into the pGreenII 0800-LUC vector to drive the firefly luciferase gene. p2GWY7-HY5-YFP

was used as the effector construct. Arabidopsis mesophyll cell protoplasts were isolated and transfected as described previously (Yoo et al., 2007). We used a Dual Luciferase kit (Yeasen) for transient expression analysis to detect reporter activity. The Renilla luciferase gene, driven by the cauliflower mosaic virus 35S promoter, was used as an internal control. The ratio of LUC/REN was calculated as an indicator of the final transcriptional activity.

Chromatin immunoprecipitation (ChIP)

The ChIP assay was performed as described by Xu et al. (2016). Chromatin isolation was performed using Col-0 and *HA-HY5 hy5-215* transgenic seedlings grown under constant white light for 4 d. The resuspended chromatin was sonicated at 4°C to 250-500 bp fragments. The sheared chromatin was immunoprecipitated, washed, and reverse cross linked. About 10% of sonicated but non-immunoprecipitated chromatin was reverse cross linked and used as an input DNA control. Monoclonal anti-HA antibody (ab9110, Abcam, 1:100 dilution) was used for immunoprecipitation. Both immunoprecipitated DNA and input DNA were analyzed by RT-PCR. The level of binding was calculated as the ratio between the IP and Input groups.

***In vitro* pull-downs**

The full-length coding sequences of *GLK1*, *GLK2*, *GNC*, and *CGA1* were cloned into pGEX-6P-1 vector, and the full-length coding sequences of *HY5* and *nDET1* (26-87 aa) were cloned into pCold-TF vector. Two mL of transformed bacteria cultures were grown over night, diluted 1:100 in the next morning, and grown for another 3 hours at 37°C. When the cells reached logarithmic phase, 0.1 mM IPTG was added to induce the expression of proteins at 37°C for 4 hours. Then 0.5 mL of each selected *E. coli* cultures was added in the same tube, re-suspended in

lysis buffer (1 × PBS, pH 7.4, 1 × complete protease inhibitor cocktail), and the cells were broken with a sonicator for 3 times (30 s on and 60 s off) on ice. After the cell debris were removed by centrifugation at 18000 g for 30 min, 20 μL Glutathione Sepharose 4B was added to the mixture sample and rotated at 4°C for 6 hours. After 4 washes with PBST buffer (1 × PBS, pH 7.4, 0.1% Triton X-100), the pellet fraction was boiled in 5 × SDS protein loading buffer, and the input and pull-down prey proteins were detected by immunoblot using anti-His (M201, Takara, 1:3000 dilution) and anti-GST (G018, Abcam, 1:3000 dilution) antibodies respectively.

Bi-luminescence complementation (BiLC) assay

GLK or HY5 was fused to the N- or C-terminus of firefly luciferase, and the constructs were transformed into agrobacterium (*Agrobacterium tumefaciens*) strain GV3101. Overnight cultures of agrobacteria were collected by centrifugation at 4000 g for 10 min, re-suspended in MES buffer (10 mM MES,10 mM $MgCl_2$, and 100 mM acetosyringone), mixed with GV3101 colonies expressing pSoup-P19 to a final OD_{600} = 0.5, and incubated at room temperature for 3 h in the dark before infiltration. The agrobacterium suspension in a 1 mL syringe (without the metal needle) was carefully press-infiltrated onto healthy leaves of 3-week-old *N. benthamiana*. The infiltrated plants were returned to long-day conditions for 3 d. Leaves were infiltrated with luciferin solution and left for 10 min, before observing luciferase activity by imaging with a CCD camera (Tanon-5200, BioTanon, China).

Co-immunoprecipitations (Co-IPs)

Arabidopsis mesophyll cell protoplasts isolated from two-week-old Col-0 plants grown in long-day conditions were used for co-IP experiments. The

712 protoplasts were transfected with a total of 10 μg DNA (p2GWY7-YFP,
713 p2GWY7-HY5-YFP, and 35S-GLK2-2XFLAG-hcf) and incubated overnight. The
714 transfected samples were spun for 2 min at 100 g, separated from the
715 supernatant, and then homogenized in binding buffer (25 mM Tris-HCl, pH 7.5, 1%
716 [v/v] Triton X-100, 150 mM NaCl, 1 mM EDTA, 10% [v/v] glycerol, and 1× protease
717 inhibitor cocktail [Roche]) by rotating at 4 °C for 1 h. The insoluble material was
718 removed by centrifugation at 13,000 g for 10 min at 4 °C, and the supernatant was
719 mixed with 40 μL of ANTI-FLAG M2 affinity beads (Sigma-Aldrich). The mixtures
720 were incubated overnight at 4 °C for 6 h, and the beads were washed three times
721 with washing buffer (25 mM Tris-HCl, pH 7.5, 0.5% [v/v] Triton X-100, 150 mM
722 NaCl, 1 mM EDTA, and 10% [v/v] glycerol). We eluted the bound proteins from the
723 affinity beads with 2× SDS-PAGE sample buffer and analyzed the eluates by
724 immunoblotting with anti-GFP (SAB4301138, Sigma-Aldrich, USA, 1:1,000
725 dilution), anti-FLAG (F1804, Sigma-Aldrich, USA, 1:5,000 dilution), and anti-Actin
726 (LF208, Epizyme Biotech, China, 1:3,000 dilution) antibodies to detect the target
727 proteins.
728
729 **RNA-seq analysis**
730 Total RNA was extracted from 4-d-old Col-0, *glk2*, *hy5*, and *hy5 glk2* seedlings
731 grown in constant white light (100 μmol photons m^{-2} s^{-1}). Sequencing libraries
732 were generated with three independent biological replicates for each material, and
733 the sequencing was performed using Illumina platform by Biomarker company
734 (Beijing). Differentially expressed genes (DEGs) were identified using DESeq
735 (Version1.18.0) (Anders et al., 2013).
736
737 **Accession numbers**
738 Sequence information from this article can be found in The Arabidopsis

Information Resource (TAIR) under the following accession numbers: *GLK1* (AT2G20570), *GLK2* (AT5G44190), *GNC* (AT5G56860), *CGA1* (AT4G26150), *DET1* (AT4G10180), *HY5* (At5G11260), *ACT7* (At5G09810), *HEMA1* (AT1G58290), *PORB* (AT4G27440), *PORC* (AT1G03630), *CAO* (AT1G44446), *LHCB1.2* (AT1G29910), *LHCB2.2* (AT2G05070), *LHCA1* (AT3G54890), *LHCA4* (AT3G47470), *EXPA5* (AT3G29030), *IAA19* (AT3G15540), *SAUR20* (AT5G18020), *PME16* (AT2G43050), *IAA7* (AT3G23050), and *XTH4* (AT2G06850).

Supplemental data

Supplemental Figure S1. HY5, GLK, GNC and CGA1 regulate the chlorophyll biosynthesis.

Supplemental Figure S2. Phenotypes of the mutants and overexpression lines under continuous white light conditions.

Supplemental Figure S3. GLK inhibits hypocotyl elongation.

Supplemental Figure S4. GNC and CGA1 promote hypocotyl elongation.

Supplemental Figure S5. HY5 but not GLKs is crucial for the greening of detached roots.

Supplemental Figure S6. 6-BA promotes GLK and HY5 dependent chlorophyll biosynthesis.

Supplemental Figure S7. Different expression patterns of HY5 and GLK2 regulated photosystem genes.

Supplemental Figure S8. *In vitro* evidence of DET1 interacting with GLK and GNC/CGA1.

Supplemental Dataset 1. List of 516 GLK2 regulated genes.

Supplemental Dataset 2. List of 656 HY5 regulated genes.

Supplemental Dataset 3. List of 716 HY5 and GLK2 regulated genes.

Supplemental Data 4. Primers used in this study.

Supplemental Data 5. Statistical analysis for the data shown in figures.

Acknowledgments

We thank Prof. Jane Langdale for comments and suggestions on the work. We thank Xiao-Yan Gao and Zhi-Ping Zhang for technical support on the transmission electron microscopy. We are grateful to Prof. Hong-Hui Lin for kindly providing the AtGLK1 antibody; Chun-Guang Chen from ORIZYMES for generating the AtGLK2 antibody; Prof. G. Eric Schaller for gift of Arabidopsis GNC/CGA1 mutants and overexpression lines.

Funding

This work was supported by the National Natural Science Foundation of China (No. 31970257).

References

Abbas N, Maurya JP, Senapati D, Gangappa SN, and Chattopadhyay S (2014) Arabidopsis CAM7 and HY5 physically interact and directly bind to the HY5 promoter to regulate its expression and thereby promote photomorphogenesis. Plant Cell **26:** 1036–1052

Alem AL, Ariel FD, Cho Y, Hong JC, Gonzalez DH, and Viola IL (2022) TCP15 interacts with GOLDEN2-LIKE 1 to control cotyledon opening in Arabidopsis. Plant J **110(3):** 748–763

Anders S and Hubre W (2013) Differential expression of RNA-Seq data at the gene level-the DESeq package. European Molecular Biology Laboratory (EMBL)

Arnon DI (1949) Copper enzymes in isolated chloroplasts polypheoloxidase in Bata Vulgaris. Plant Physiol **24:** 1–15

Bastakis E, Hedtke B, Klermund C, Grimm B, and Schwechheimer, C (2018) LLM-Domain B-GATA transcription factors play multifaceted roles in controlling greening in Arabidopsis. Plant Cell **30:** 582–599

Bi YM, Zhang Y, Signorelli T, Zhao R, Zhu T, and Rothstein S (2005) Genetic analysis of Arabidopsis GATA transcription factor gene family reveals a nitrate-inducible member important for chlorophyll synthesis and glucose sensitivity. Plant J **44:** 680–692

Binkert M, Kozma-Bognár L, Terecskei K, De Veylder L, Nagy F, and Ulm R (2014) UV-B-responsive association of the Arabidopsis bZIP transcription factor ELONGATED HYPOCOTYL5 with target genes, including its own promoter. Plant Cell **26:** 4200–4213

Catalá R, Medina J, and Salinas J (2011) Integration of low temperature and light signaling during cold acclimation response in Arabidopsis. Proc Natl Acad Sci USA **108:** 16475–16480

Chang CS, Li YH, Chen LT, Chen WC, Hsieh WP, Shin J, Jane WN, Chou SJ, Choi G, Hu JM, Somerville S, and Wu SH (2008) LZF1, a HY5-regulated transcriptional factor, functions in Arabidopsis de-etiolation. Plant J **54:** 205–219

Chen D, Xu G, Tang W, Jing Y, Ji Q, Fei Z, and Lin R (2013) Antagonistic basic helix-loop-helix/bZIP transcription factors form transcriptional modules that integrate light and reactive oxygen species signaling in Arabidopsis. Plant Cell **25:** 1657–1673

Chiang YH, Zubo YO, Tapken W, Kim HJ, Lavanway AM, Howard L, Pilon M, Kieber JJ, and Schaller GE (2012) Functional characterization of the GATA transcription factors GNC and CGA1 reveals their key role in chloroplast development, growth, and division in Arabidopsis. Plant Physiol **160:** 332–348

Chory J, Peto C, Feinbaum R, Pratt L, and Ausubel F (1989) Arabidopsis thaliana mutant that develops as a light-grown plant in the absence of light. Cell **58:** 991–999

Ciolfi A, Sessa G, Sassi M, Possenti M, Salvucci S, Carabelli M, Morelli G, and Ruberti I (2013) Dynamics of the shade-avoidance response in Arabidopsis. Plant Physiol **163:** 331–353

Datta S, Hettiarachchi C, Johansson H, and Holm M (2007) SALT TOLERANCE HOMOLOG2, a B-box protein in Arabidopsis that activates transcription and positively regulates light-mediated development. Plant Cell **19:** 3242–3255

Datta S, Johansson H, Hettiarachchi C, Irigoyen ML, Desai M, Rubio V, and Holm M (2008) LZF1/SALT TOLERANCE HOMOLOG3, an Arabidopsis B-box protein involved in light-dependent development and gene expression, undergoes COP1-mediated ubiquitination. Plant Cell **20:** 2324–2338

Deng XW, Matsui M, Wei N, Wagner D, Chu AM, Feldmann KA, and Quail PH (1992) COP1, an Arabidopsis regulatory gene, encodes a protein with both a zinc-binding motif and a G beta homologous domain. Cell **71:** 791–801

Fitter DW, Martin DJ, Copley MJ, Scotland RW, and Langdale JA (2002) GLK gene pairs regulate chloroplast development in diverse plant species. Plant J **31:** 713–727

Hall LN, Rossini L, Cribb L, and Langdale JA (1998) GOLDEN 2: a novel transcriptional regulator of cellular differentiation in the maize leaf. Plant Cell **10:** 925–936

Holm M, Ma LG, Qu LJ, and Deng XW (2002) Two interacting bZIP proteins are direct targets of COP1-mediated control of light-dependent gene expression in Arabidopsis. Genes Dev **16:** 1247–1259

Huang X, Ouyang X, Yang P, Lau OS, Li G, Li J, Chen H, and Deng XW (2012)

Arabidopsis FHY3 and HY5 positively mediate induction of COP1 transcription in response to photomorphogenic UV-B light. Plant Cell **24:** 4590–4606

Hudson D, Guevara DR, Hand AJ, Xu Z, Hao L, Chen X, Zhu T, Bi YM, and Rothstein SJ (2013). Rice cytokinin GATA transcription Factor1 regulates chloroplast development and plant architecture. Plant Physiol **162:** 132–144

Imamura A, Hanaki N, Nakamura A, Suzuki T, Taniguchi M, Kiba T, Ueguchi C, Sugiyama T, and Mizuno T (1999) Compilation and characterization of Arabidopsis thaliana response regulators implicated in His-Asp phosphorelay signal transduction. Plant Cell Physiol **40:** 733–742

Jakoby M, Weisshaar B, Dröge-Laser W, Vicente-Carbajosa J, Tiedemann J, Kroj T, Parcy F, and bZIP Research Group (2002) bZIP transcription factors in Arabidopsis. Trends Plant Sci **7:** 106–111

Jang IC, Henriques R, and Chua NH (2013) Three transcription factors, HFR1, LAF1 and HY5, regulate largely independent signaling pathways downstream of phytochrome A. Plant Cell Physiol **54:** 907–916

Jiao Y, Lau OS, and Deng XW (2007) Light-regulated transcriptional networks in higher plants. Nat Rev Genet **8:** 217–230

Jing Y, Zhang D, Wang X, Tang W, Wang W, Huai J, Xu G, Chen D, Li Y, and Lin R (2013) Arabidopsis chromatin remodeling factor PICKLE interacts with transcription factor HY5 to regulate hypocotyl cell elongation. Plant Cell **25:** 242–256

Kobayashi K, Baba S, Obayashi T, Sato M, Toyooka K, Keränen M, Aro EM, Fukaki H, Ohta H, Sugimoto K, and Masuda T (2012a) Regulation of root greening by light and auxin/cytokinin signaling in Arabidopsis. Plant Cell **24:** 1081–1095

Kobayashi K, Obayashi T, and Masuda T (2012b) Role of the G-box element in

regulation of chlorophyll biosynthesis in Arabidopsis roots. Plant Signal Behav **7:** 922–926

Kobayashi K, Ohnishi A, Sasaki D, Fujii S, Iwase A, Sugimoto K, Masuda T, and Wada H (2017) Shoot Removal Induces Chloroplast Development in Roots via Cytokinin Signaling. Plant Physiol **173:** 2340–2355

Kushwaha R, Singh A, and Chattopadhyay S (2008) Calmodulin7 plays an important role as transcriptional regulator in Arabidopsis seedling development. Plant Cell **20:** 1747–1759

Lee D, Hua L, Khoshravesh R, Giuliani R, Kumar I, Cousins A, Sage TL, Hibberd JM, and Brutnell TP (2021) Engineering chloroplast development in rice through cell‐specific control of endogenous genetic circuits. Plant Biotechnol J **19(11):** 2291–2303

Lee J, Choi B, Yun A, Son N, Ahn G, Cha JY, Kim WY, and Hwang I (2021) Long-term abscisic acid promotes golden2-like1 degradation through constitutive photomorphogenic 1 in a light intensity-dependent manner to suppress chloroplast development. Plant Cell Environ **44:** 3034–3048

Lee J, He K, Stolc V, Lee H, Figueroa P, Gao Y, Tongprasit W, Zhao H, Lee I, and Deng XW (2007) Analysis of transcription factor HY5 genomic binding sites revealed its hierarchical role in light regulation of development. Plant Cell **19:** 731–749

Liu D, Zhao D, Li X, and Zeng YJ (2022) AtGLK2, an Arabidopsis GOLDEN2-LIKE transcription factor, positively regulates anthocyanin biosynthesis via AtHY5-mediated light signaling. Plant Growth Regul **96:** 79–90

Martín G, Leivar P, Ludevid D, Tepperman JM, Quail PH, and Monte E (2016) Phytochrome and retrograde signalling pathways converge to antagonistically regulate a light-induced transcriptional network. Nat

Commun **7:** 11431

Naito T, Kiba T, Koizumi N, Yamashino T, and Mizuno T (2007) Characterization of a unique GATA family gene that responds to both light and cytokinin in Arabidopsis thaliana. Biosci Biotechnol Biochem **71:** 1557–1560

Nakamura H, Muramatsu M, Hakata M, Ueno O, Nagamura Y, Hirochika H, Takano M, and Ichikawa H (2009) Ectopic overexpression of the transcription factor OsGLK1 induces chloroplast development in non-green rice cells. Plant Cell Physiol **50:** 1933–1949

Nguyen CV, Vrebalov JT, Gapper NE, Zheng Y, Zhong S, Fei Z, and Giovannoni JJ (2014) Tomato GOLDEN2-LIKE transcription factors reveal molecular gradients that function during fruit development and ripening. Plant Cell **26:** 585–601

Osterlund MT, Hardtke CS, Wei N, and Deng XW (2000) Targeted destabilization of HY5 during light-regulated development of Arabidopsis. Nature **405:** 462–466

Oyama T, Shimura Y, and Okada K (1997) The Arabidopsis HY5 gene encodes a bZIP protein that regulates stimulus-induced development of root and hypocotyl. Genes Dev **11:** 2983–2995

Ram H, Priya P, Jain M, and Chattopadhyay S (2014) Genome-wide DNA binding of GBF1 is modulated by its heterodimerizing protein partners, HY5 and HYH. Mol Plant **7:** 448–451

Ranftl QL, Bastakis E, Klermund C, and Schwechheimer C (2016) LLM-Domain Containing B-GATA Factors Control Different Aspects of Cytokinin-Regulated Development in Arabidopsis thaliana. Plant Physiol **170(4):** 2295–2311

Rauf M, Arif M, Dortay H, Matallana-Ramírez LP, Waters MT, Gil Nam H, Lim

PO, Mueller-Roeber B, and Balazadeh S (2013) ORE1 balances leaf senescence against maintenance by antagonizing G2-like-mediated transcription. Embo Rep **14:** 382–388

Rossini L, Cribb L, Martin DJ, and Langdale JA (2001) The maize golden2 gene defines a novel class of transcriptional regulators in plants. Plant Cell **13:** 1231–1244

Saijo Y, Sullivan JA, Wang H, Yang J, Shen Y, Rubio V, Ma L, Hoecker U, and Deng XW (2003) The COP1-SPA1 interaction defines a critical step in phytochrome A-mediated regulation of HY5 activity. Genes Dev **17:** 2642–2647

Seo HS, Yang JY, Ishikawa M, Bolle C, Ballesteros ML, and Chua NH (2003) LAF1 ubiquitination by COP1 controls photomorphogenesis and is stimulated by SPA1. Nature **423:** 995–999

Shin J, Park E, and Choi G (2007) PIF3 regulates anthocyanin biosynthesis in an HY5-dependent manner with both factors directly binding anthocyanin biosynthetic gene promoters in Arabidopsis. Plant J **49:** 981–994

Singh A, Ram H, Abbas N, and Chattopadhyay S (2012) Molecular interactions of GBF1 with HY5 and HYH proteins during light-mediated seedling development in Arabidopsis thaliana. J Biol Chem **287:** 25995–26009

Song Y, Yang C, Gao S, Zhang W, Li L, and Kuai B (2014) Age-triggered and dark-induced leaf senescence require the bHLH transcription factors PIF3, 4, and 5. Mol Plant **7:** 1776–1787

Stracke R, Favory JJ, Gruber H, Bartelniewoehner L, Bartels S, Binkert M, Funk M, Weisshaar B, and Ulm R (2010) The Arabidopsis bZIP transcription factor HY5 regulates expression of the PFG1/MYB12 gene in response to light and ultraviolet-B radiation. Plant Cell Environ **33:** 88–103

Sullivan JA and Deng XW (2003) From seed to seed: the role of photoreceptors

in Arabidopsis development. Dev Biol **260:** 289–297

Tamai H, Iwabuchi M, and Meshi T (2002) Arabidopsis GARP transcriptional activators interact with the Pro-rich activation domain shared by G-box-binding bZIP factors. Plant Cell Physiol **43:** 99–107

Tang X, Miao M, Niu X, Zhang D, Cao X, Jin X, Zhu Y, Fan Y, Wang H, Liu Y, Sui Y, Wang W, Wang A, Xiao F, Giovannoni J, and Liu Y (2016) Ubiquitin-conjugated degradation of golden 2-like transcription factor is mediated by CUL4-DDB1-based E3 ligase complex in tomato. New Phytol **209:** 1028–1039

Tepperman JM, Hwang Y-S, and Quail PH (2006) phyA dominates in transduction of red-light signals to rapidly responding genes at the initiation of Arabidopsis seedling de-etiolation. Plant J **48:** 728–742

Tokumaru M, Adachi F, Toda M, Ito-Inaba Y, Yazu F, Hirosawa Y, Sakakibara Y, Suiko M, Kakizaki T, and Inaba T (2017) Ubiquitin-Proteasome Dependent Regulation of the GOLDEN2-LIKE 1 Transcription Factor in Response to Plastid Signals. Plant Physiol **173:** 524–535

Toledo-Ortiz G, Johansson H, Lee KP, Bou-Torrent J, Stewart K, Steel G, Rodríguez-Concepción M, and Halliday KJ (2014) The HY5-PIF regulatory module coordinates light and temperature control of photosynthetic gene transcription. PLoS Genet **10:** e1004416

Waters MT, Moylan EC, and Langdale JA (2008) GLK transcription factors regulate chloroplast development in a cell-autonomous manner. Plant J **56:** 432–444

Waters MT, Wang P, Korkaric M, Capper RG, Saunders NJ, and Langdale JA (2009) GLK transcription factors coordinate expression of the photosynthetic apparatus in Arabidopsis. Plant Cell **21:** 1109–1128

Wykoff DD, Grossman AR, Weeks DP, Usuda H, and Shimogawara K (1999)

Psr1, a nuclear localized protein that regulates phosphorus metabolism in Chlamydomonas. Proc Natl Acad Sci USA **96:** 15336–15341

Xu D, Jiang Y, Li J, Lin F, Holm M, and Deng XW (2016a) BBX21, an Arabidopsis B-box protein, directly activates HY5 and is targeted by COP1 for 26S proteasome-mediated degradation. Proc Natl Acad Sci USA **113:** 7655–7660

Xu X, Chi W, Sun X, Feng P, Guo H, Li J, Lin R, Lu C, Wang H, Leister D, and Zhang L (2016b) Convergence of light and chloroplast signals for de-etiolation through ABI4-HY5 and COP1. Nat Plants **2:** 16066

Xu Z, Casaretto JA, Bi YM, and Rothstein SJ (2017) Genome-wide binding analysis of AtGNC and AtCGA1 demonstrates their cross-regulation and common and specific functions. Plant Direct **1:** e00016

Yang J, Lin R, Sullivan J, Hoecker U, Liu B, Xu L, Deng XW, and Wang H (2005) Light regulates COP1-mediated degradation of HFR1, a transcription factor essential for light signaling in Arabidopsis. Plant Cell **17:** 804–821

Yoo SD, Cho YH, and Sheen J (2007) Arabidopsis mesophyll protoplasts: a versatile cell system for transient gene expression analysis. Nat Protoc **2(7):** 1565–1572

Zhang D, Tan W, Yang F, Han Q, Deng X, Guo H, Liu B, Yin Y, and Lin H (2021) A BIN2-GLK1 Signaling Module Integrates Brassinosteroid and Light Signaling to Repress Chloroplast Development in the Dark. Dev Cell **56:** 310–324 e317

Zhang H, He H, Wang X, Wang X, Yang X, Li L, and Deng XW (2011) Genome-wide mapping of the HY5-mediated gene networks in Arabidopsis that involve both transcriptional and post-transcriptional regulation. Plant J **65:** 346–358

Zhao YR, Li X, Yu KQ, Cheng F, and He Y (2016) Hyperspectral Imaging for

Determining Pigment Contents in Cucumber Leaves in Response to Angular Leaf Spot Disease. Sci Rep **6:** 27790

Zubo YO, Blakley IC, Franco-Zorrilla JM, Yamburenko MV, Solano R, Kieber JJ, Loraine AE, and Schaller GE (2018) Coordination of Chloroplast Development through the Action of the GNC and GLK Transcription Factor Families. Plant Physiol **178:** 130–147

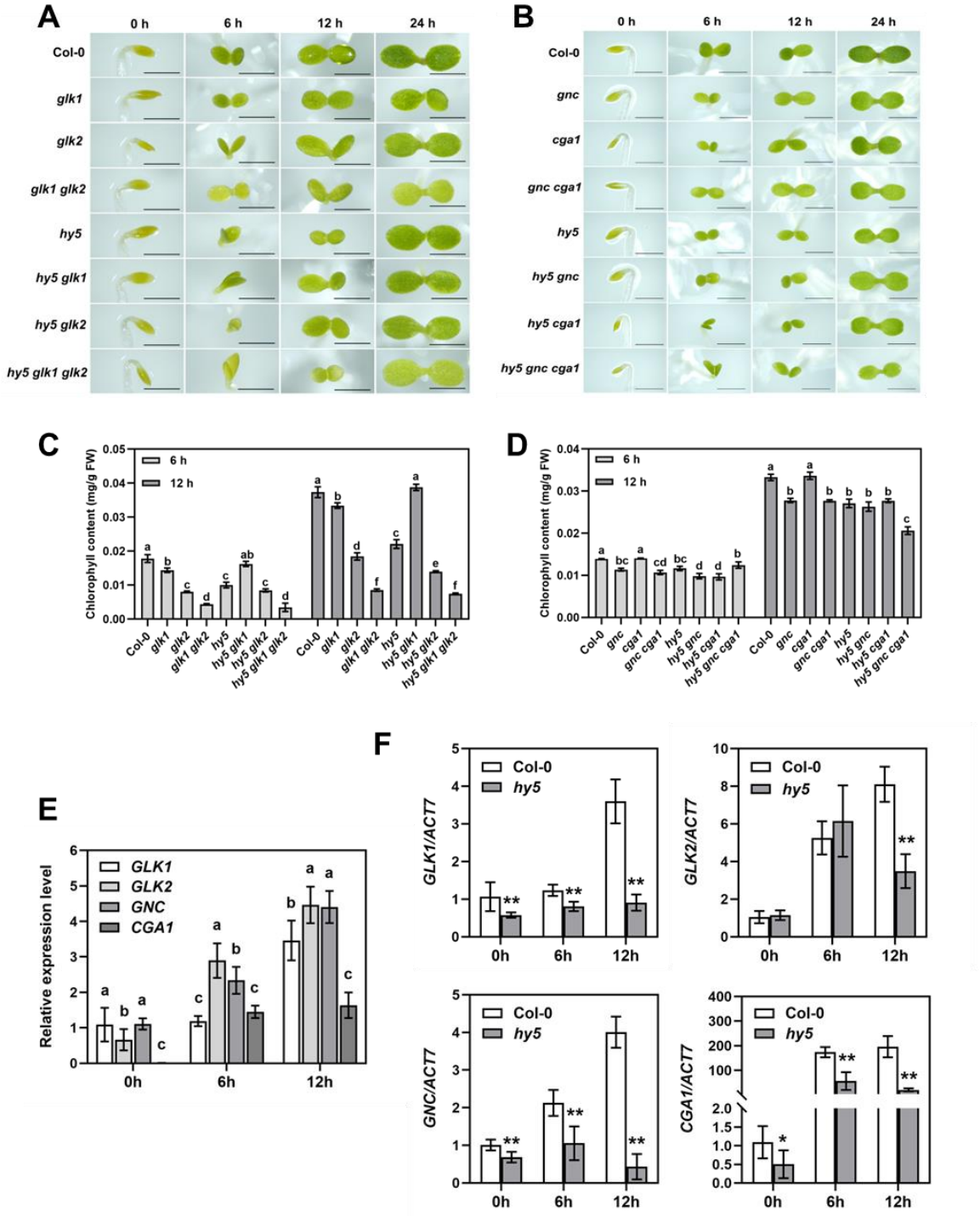

Figure 1. GLK1/2 and GNC/CGA1 positively regulate chlorophyll content downstream of HY5 during de-etiolation.

(A) Phenotypes of 4-day-old etiolated seedlings of Col-0, *glk1*, *glk2*, *glk1 glk2*, *hy5*,

hy5 glk1, *hy5 glk2*, and *hy5 glk1 glk2* during transition from dark to light conditions for 6 h, 12 h, 24 h. Scale bars = 1 mm.

(B) Phenotypes of 4-day-old etiolated seedlings of Col-0, *gnc*, *cga1*, *gnc cga1*, *hy5*, *hy5 gnc*, *hy5 cga1*, and *hy5 gnc cga1* during transition from dark to light conditions for 6 h, 12 h, 24 h. Scale bars = 1 mm.

(C, D) Chlorophyll contents of de-etiolating seedlings during transition from (A) and (B) dark to light for 6 h and 12 h. The data represent means ± SD (n = 3) and letters above the bars indicate significant differences ($P < 0.05$), as determined by one-way ANOVA with Turkey's HSD test.

(E) The expression levels of *GLK1*, *GLK2*, *GNC* and *CGA1* in 4-d-old dark-grown Col-0 upon being transferred to white light at indicated time points. The *ACT7* gene was used as internal control. The data represent means ± SD (n = 3) and letters above the bars indicate significant differences ($P < 0.05$), as determined by one-way ANOVA with Turkey's HSD test.

(F) The expression levels of *GLK1*, *GLK2*, *GNC* and *CGA1* in 4-d-old dark-grown Col-0 and *hy5* seedlings upon being transferred to white light at indicated time points. The data represent means ± SD (n = 3), and asterisks indicate a significant difference compared with Col-0 (*P<0.05, **P<0.01, paired samples *t*-test).

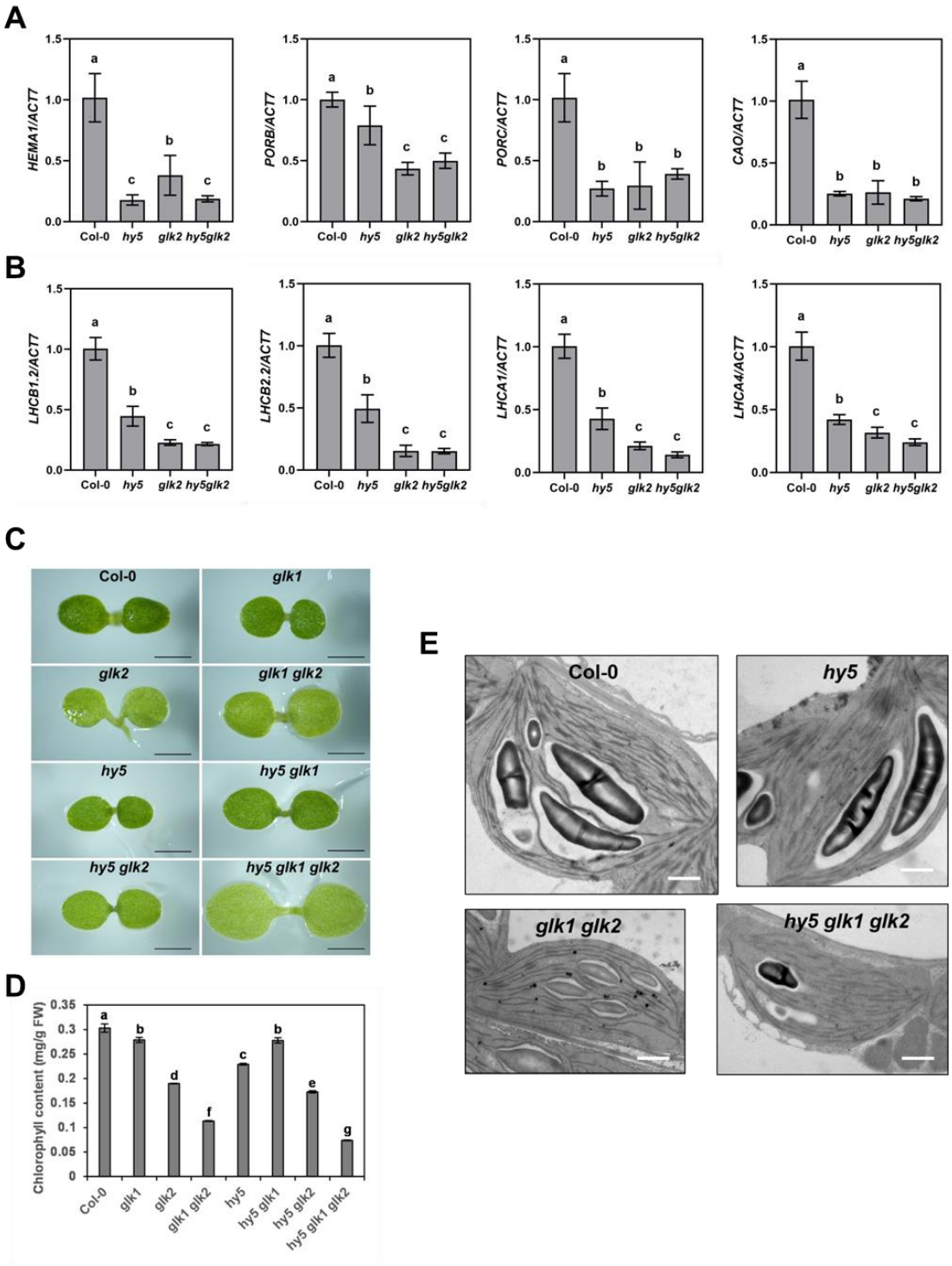

Figure 2. Chloroplast development and photosynthetic gene expression is further impaired in *hy5* and *glk* multiple mutants.

(A, B) RT-qPCR analysis of chlorophyll biosynthesis and photosystem genes

expressed in 4-d-old etiolated seedlings of Col-0, *hy5*, *glk2* and *hy5 glk2* upon being transferred to white light for 12 h. The *ACT7* gene was used as internal control. The data represent means ± SD (n = 3) and letters above the bars indicate significant differences ($P < 0.05$), as determined by one-way ANOVA with Turkey's HSD test.

(C) Phenotypes of 4-day-old Col-0, *glk1*, *glk2*, *glk1 glk2*, *hy5*, *hy5 glk1*, *hy5 glk2*, and *hy5 glk1 glk2* seedlings grown on half-strength MS plates under continuous white light conditions. Scale bars = 1 mm.

(D) Chlorophyll contents of the genotypes shown in **(A)**. The data represent means ± SD (n = 3) and letters above the bars indicate significant differences ($P < 0.05$), as determined by one-way ANOVA with Turkey's HSD test.

(E) The ultrastructure of mesophyll cell chloroplasts of Col-0, *hy5*, *glk1 glk2*, and *hy5 glk1 glk2* seedlings grown under continuous white light for 7 days. Scale bar = 1 μm.

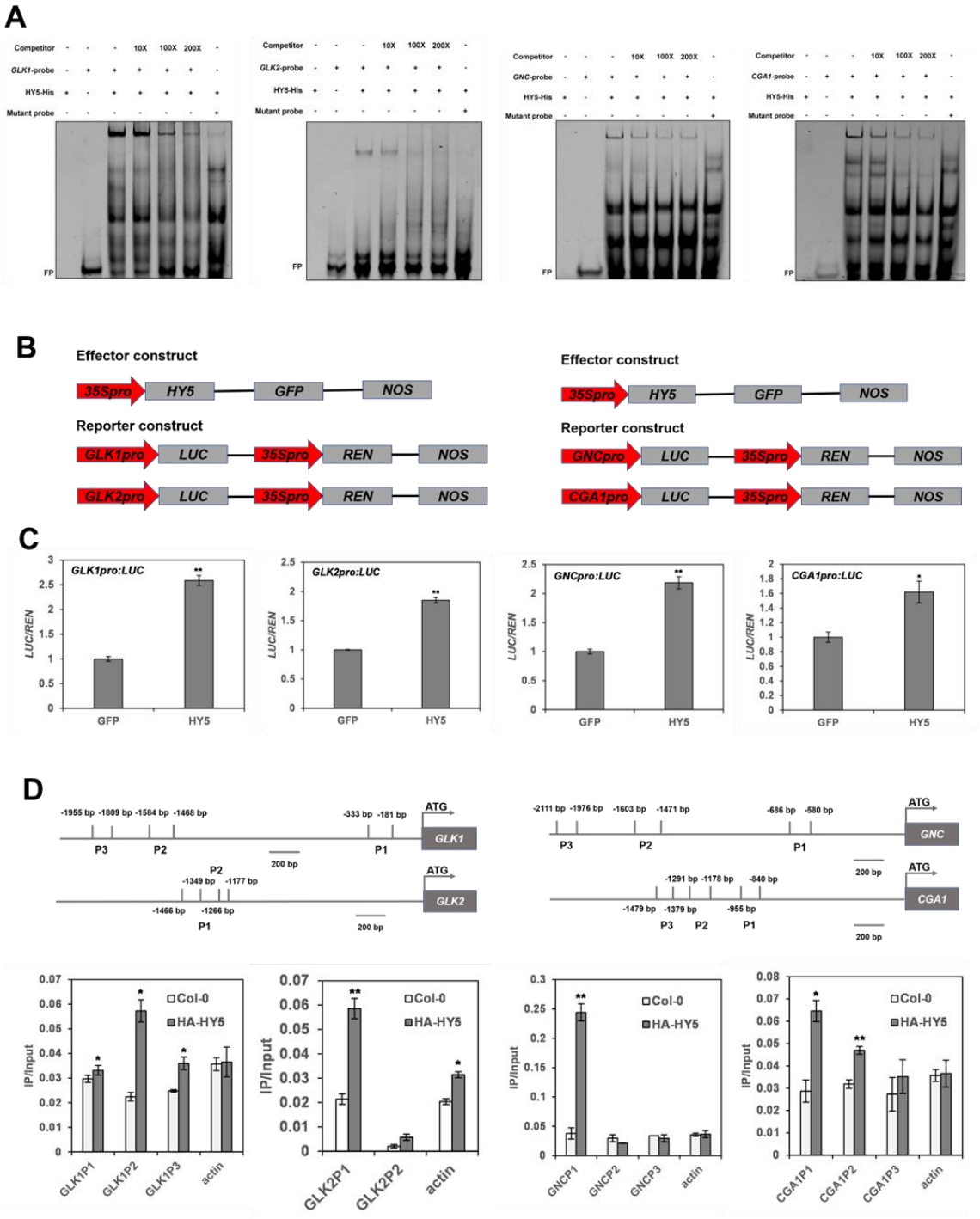

Figure 3. Binding of HY5 to the promoters and transcriptional activation of *GLK1, GLK2, GNC* and *CGA1*.

(A) EMSA showing HY5 binds to the sub-fragments of promoters of *GLK1*, *GLK2*, *GNC* and *CGA1 in vitro*. "-" and "+" indicate the absence and presence of

corresponding probes or proteins. FP means free probe.

(B) Schematic structures of effector and reporter constructs used in dual-luciferase (LUC) reporter system. *REN*, renilla luciferase gene.

(C) Bar graphs showing HY5 induces the activation of *GLK1pro:LUC*, *GLK2pro:LUC*, *GNCpro:LUC* and *CGA1pro:LUC*. The data represent means ± SD (n = 4), and asterisks indicate a significant difference compared with control (*P<0.05, **P<0.01, paired samples *t*-test).

(D) Illustration of *GLK1*, *GLK2*, *GNC* and *CGA1* promoter regions with the indicated positions of primers used in ChIP-qPCR. Bar graphs showing ChIP-qPCR assays that HY5 associates with the promoters in vivo. Col-0 material and *ACTIN* gene were used as negative controls. The data represent means ± SD (n = 3), and asterisks indicate a significant difference compared with Col-0 (*P<0.05, **P<0.01, paired samples *t*-test).

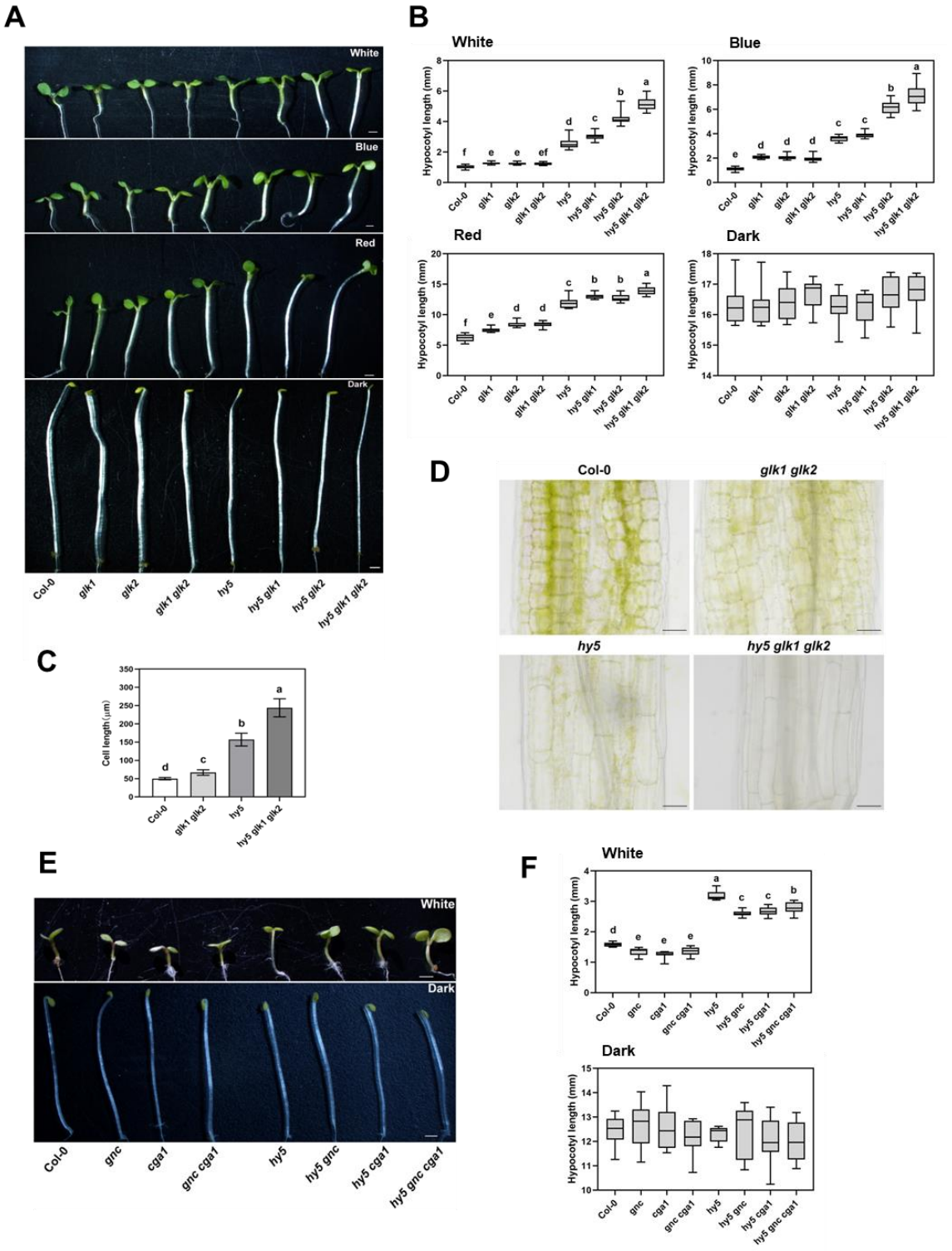

Figure 4. GLK1/2 negatively and GNC/CGA1 positively regulate hypocotyl elongation.

(A) Phenotypes of 4-d-old Col-0, *glk1*, *glk2*, *glk1 glk2*, *hy5*, *hy5 glk1*, *hy5 glk2*, and *hy5 glk1 glk2* seedlings grown in white (100 μmol/m^2/s), blue (60 μmol/m^2/s), red (90 μmol/m^2/s) light and dark conditions. Scale bar = 1 mm.

(B) Quantification of hypocotyl lengths indicated in (A). The data represent means ± SD (n ≥17) and letters above the bars indicate significant differences ($P < 0.05$), as determined by one-way ANOVA with Turkey's HSD test.

(C) Quantification of hypocotyl cell length from 4-d-old Col-0, *glk1 glk2*, *hy5*, and *hy5 glk1 glk2* seedlings, grown in white light (100 μmol/m^2/s) conditions. The data represent means ± SD (n = 15) and letters above the bars indicate significant differences ($P < 0.05$), as determined by one-way ANOVA with Turkey's HSD test.

(D) Hypocotyl cell length phenotypes from 4-d-old Col-0, *glk1 glk2*, *hy5*, and *hy5 glk1 glk2* seedlings. Scale bar = 20 μm.

(E) Phenotypes of 4-d-old Col-0, *gnc*, *cga1*, *gnc cga1*, *hy5*, *hy5 gnc*, *hy5 cga1*, and *hy5 gnc cga1* seedlings grown in white light (100 μmol/m^2/s) and dark conditions. Scale bar = 1 mm.

(F) Quantification of hypocotyl lengths indicated in (E). The data represent means ± SD (n ≥15) and letters above the bars indicate significant differences ($P < 0.05$), as determined by one-way ANOVA with Turkey's HSD test.

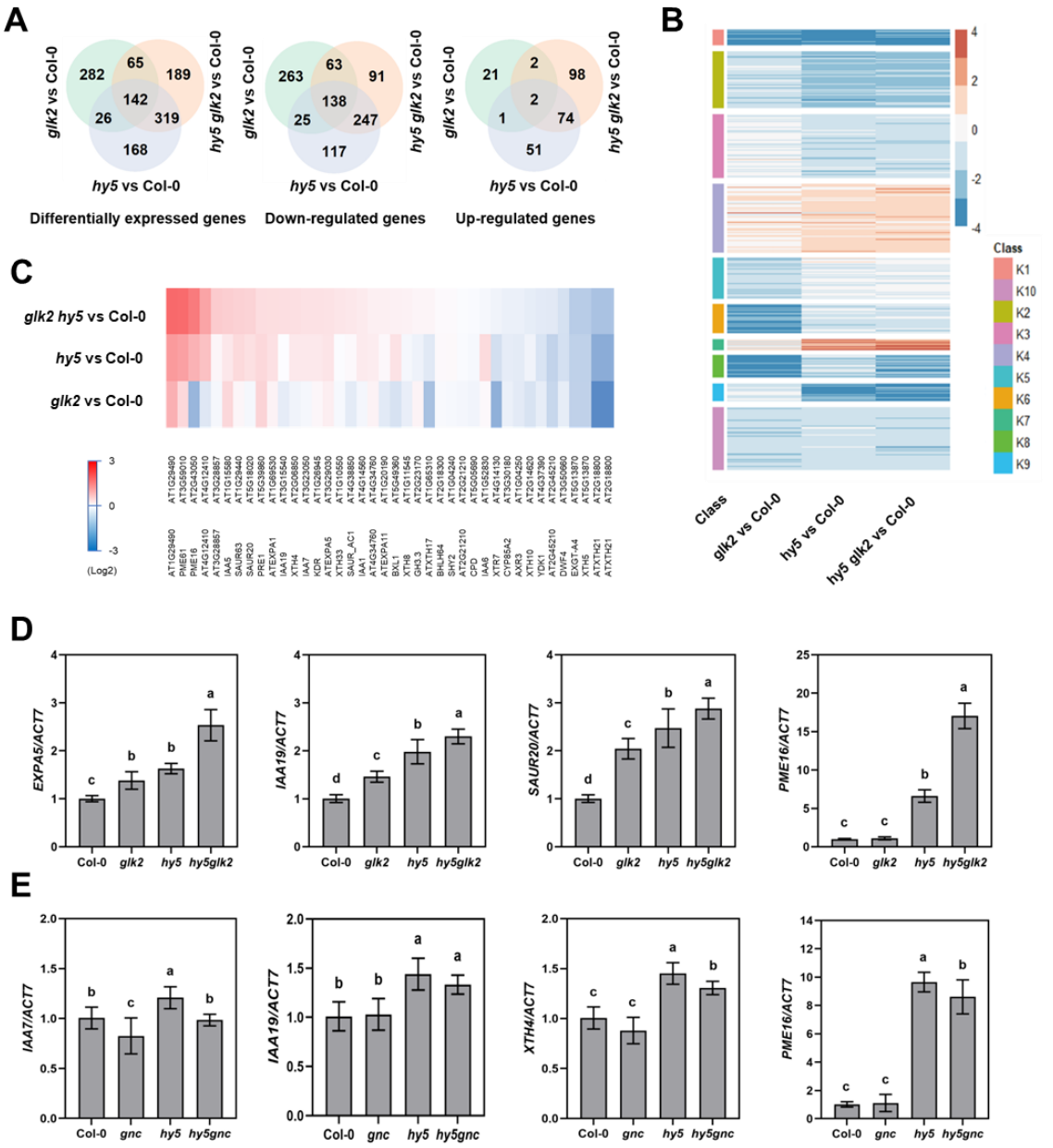

Figure 5. Different expression patterns of HY5, GLK2, and GNC regulated elongation genes.

(A) Venn diagram showing overlaps between sets of differentially expressed genes in *glk2*, *hy5* and *hy5 glk2* mutants, relative to Col-0.
(B) K-means clustering of differentially expressed genes regulated by GLK2, HY5 and both. The scale bar shows fold changes (log2 value).
(C) Expression patterns of cell elongation genes in *glk2*, *hy5* and *hy5 glk2* mutants, relative to Col-0. The scale bar shows fold changes (log2 value). Heat

map was aligned according to fold changes in *hy5 glk2* mutant.

(D, E) RT-qPCR analysis of cell elongation genes expressed in 4-d-old Col-0, *hy5*, *glk2*, *hy5 glk2*, *gnc*, and *hy5 gnc* seedlings grown under continuous white light. The *ACT7* gene was used as internal control. The data represent means ± SD (n = 3) and letters above the bars indicate significant differences ($P < 0.05$), as determined by one-way ANOVA with Turkey's HSD test.

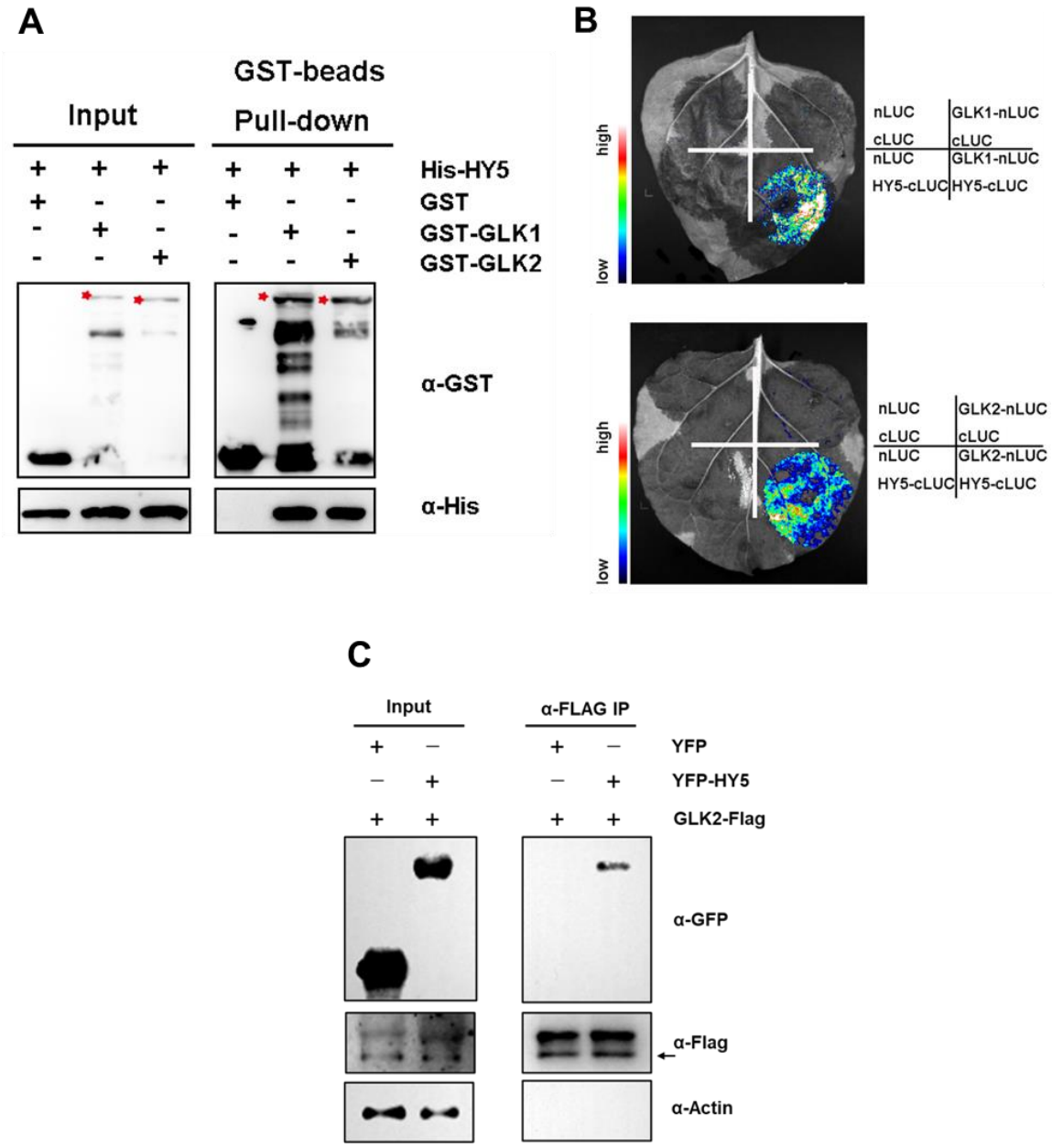

Figure 6. Evidences of HY5 interacting with GLK proteins.

(A) *In vitro* pulldown assays showing the interaction of GLK1 and GLK2 with HY5. GST-GLK protein or GST protein were used to pull down His-HY5 protein using GST beads. Anti-GST and anti-His antibodies were used for immunoblot analysis. "-" and "+" indicate the absence and presence of corresponding proteins.
(B) Bimolecular luminescence complementation assays showing GLK1 and GLK2 can interact with HY5. nLUC and cLUC served as negative controls.
(C) Co-immunoprecipitation assays using a transient expression system in

Arabidopsis mesophyll cell protoplast, showing that GLK2 interacts with HY5 *in vivo*. Protein extract was precipitated with FLAG beads, and fusion proteins were detected by immunoblot analysis using anti-GFP and anti-FLAG antibodies.

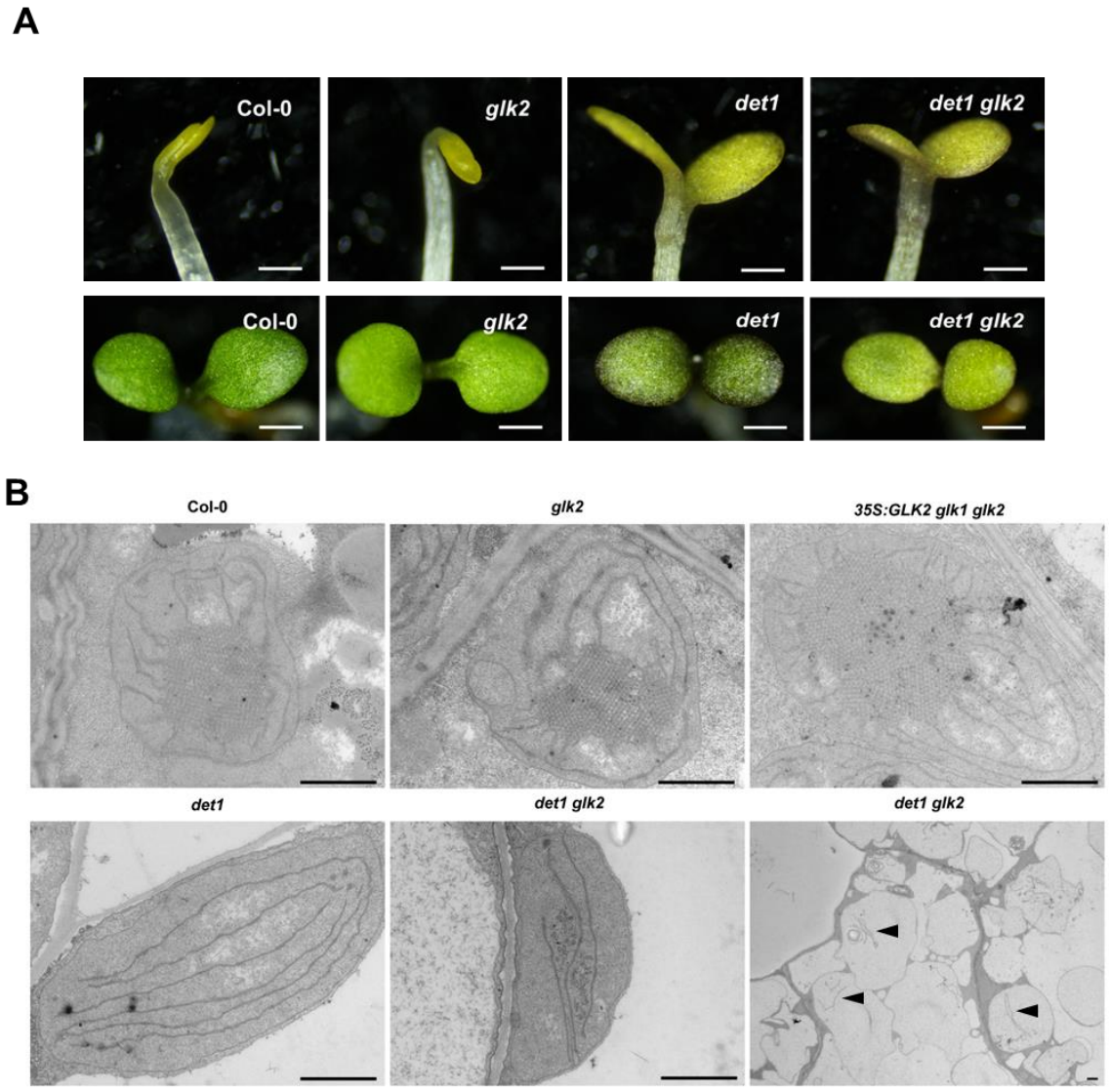

Figure 7. GLK2 is responsible for the developed thylakoid structures in the etiolated *det1* mutant.

(A) Phenotype of 4 d dark (upper panel) or light (lower panel) grown Col-0, *glk2*, *det1*, and *det1 glk2* seedlings. Scale bars represent 500 μm (upper panel) or 1 mm (lower panel).
(B) The ultrastructure of mesophyll chloroplasts of Col-0, *glk2*, *35S:GLK2 glk1 glk2*, *det1*, and *det1 glk2* seedlings grown under dark condition for 4 days. Scale bar = 1 μm. Black arrow heads in the bottom right image point to the thylakoid lamellae in very few amout.

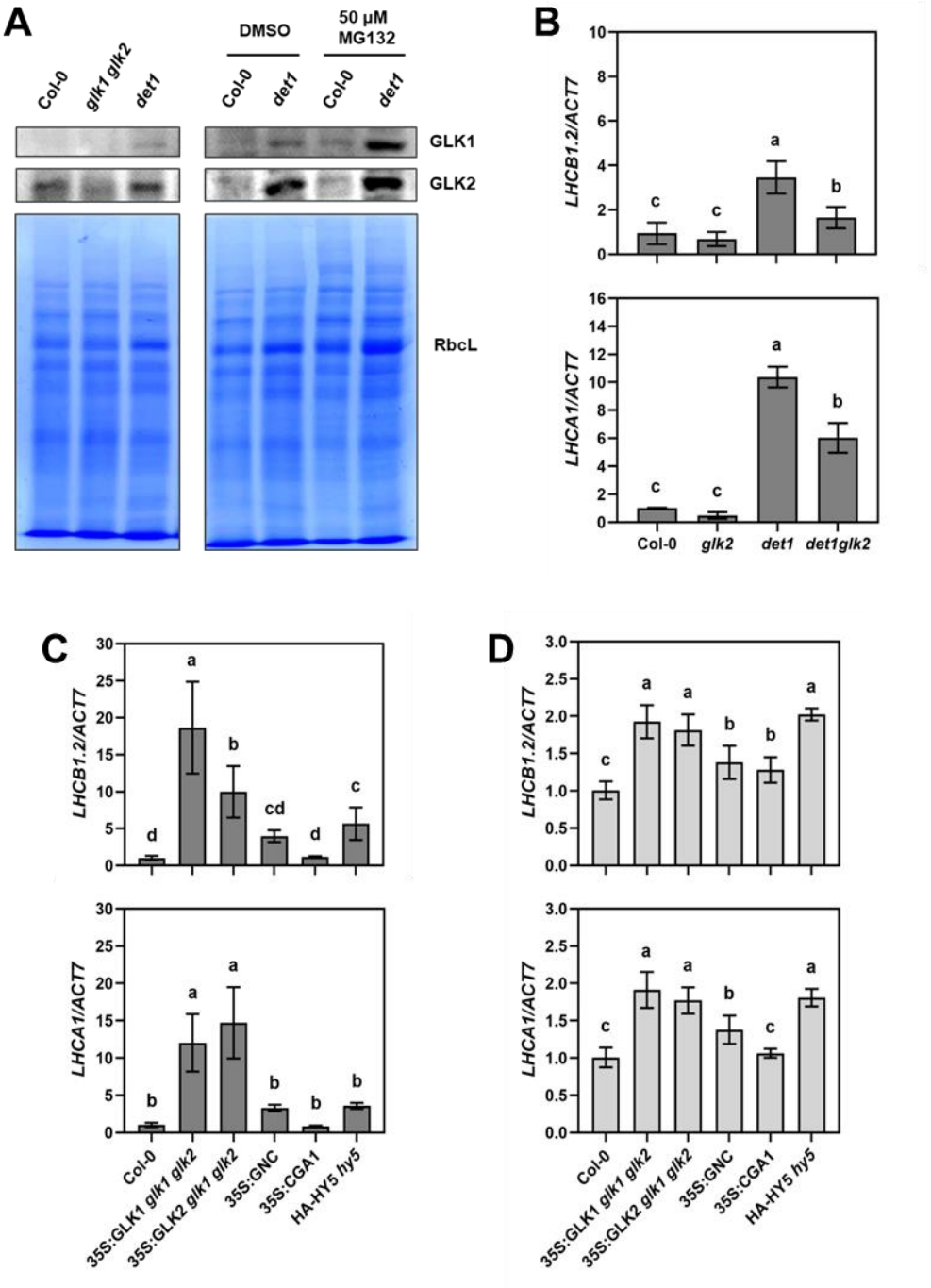

Figure 8. DET1 promotes the degradation of GLK protein, and GLK is responsible for photosystem gene expression in the etiolated *det1* mutant.

(A) Immunoblot detection of GLK1 and GLK2 in Col-0, *glk1 glk2*, and *det1* seedlings grown in the dark for 4 d (left). GLK protein levels in 4-d-old dark-grown Col-0 and *det1* seedlings after 12 h treatment with 50 μM MG132 or DMSO (right).

Coomassie stained PAGE gel was shown as loading control, and the band of Rubisco large subunit was indicated.

(**B**) RT-qPCR analysis of photosystem genes expressed in 4-d-old etiolated Col-0, *glk2*, *35S:GLK2 glk1 glk2*, *det1*, and *det1 glk2* seedlings.

(**C, D**) RT-qPCR analysis of photosystem genes expressed in 4-d-old etiolated (D) or light-grown (E) Col-0, *35S:GLK1 glk1 glk2*, *35S:GNC*, *35S:CGA1*, and *HA-HY5 hy5* seedlings. The *ACT7* gene was used as internal control. The data represent means ± SD (n = 3) and letters above the bars indicate significant differences ($P < 0.05$), as determined by one-way ANOVA with Turkey's HSD test.

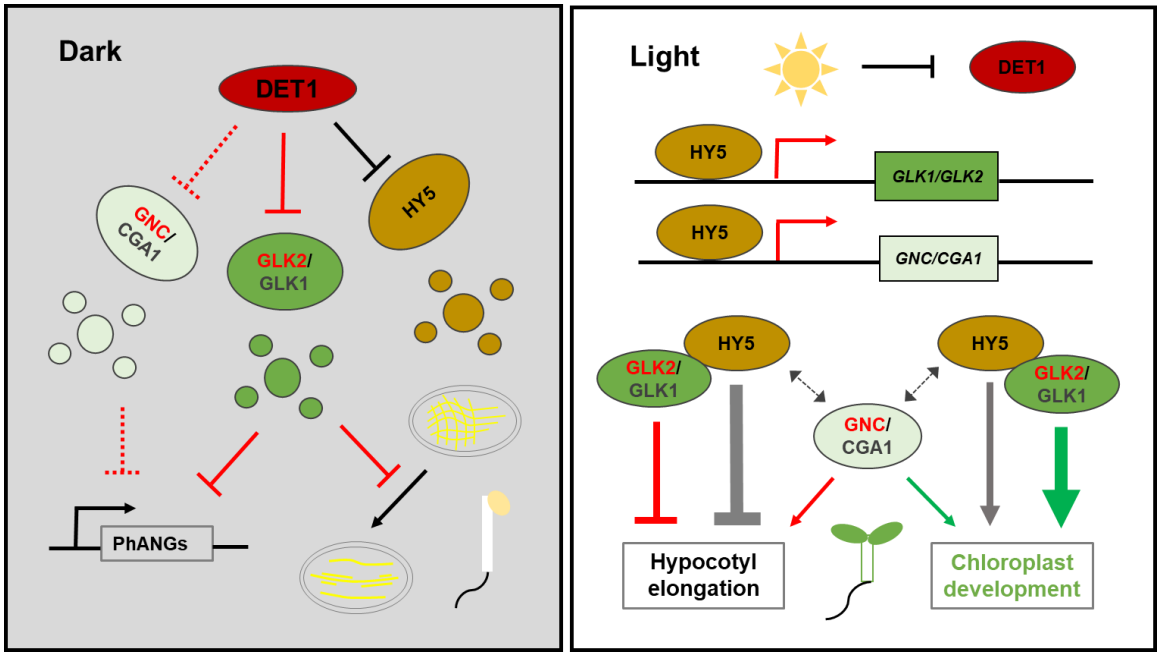

Figure 9. A working model depicting GLKs, GNC/CGA1, and HY5 in the regulation of skotomorphogenesis and photomorphogenesis.

GLKs, GNC, CGA1 and HY5 undergo DET1-mediated degradation in the dark, so that the expression of photosynthesis associated nuclear genes (PhANGs), and the transformation of prolamellar body towards extended lamellae are inhibited. Light inhibits DET1 activity, and HY5 directs the promoter of *GLKs*, *GNC* and *CGA1*, inducing their activities to promote chloroplast development. The protein interactions between HY5 and GLKs are shown. GLKs inhibit hypocotyl elongation while GNC and CGA1 promote hypocotyl elongation. Thick green arrow indicates strong promotion of chloroplast development by GLKs. Thick gray line indicates strong inhibition of hypocotyl elongation by HY5. Thinner arrows indicate less strong regulation. Dashed lines in the dark indicate GNC/CGA1 related regulations that pending to be further validated. Dashed double sided arrows in the light indicate potential protein interactions of HY5 with GNC/CGA1.

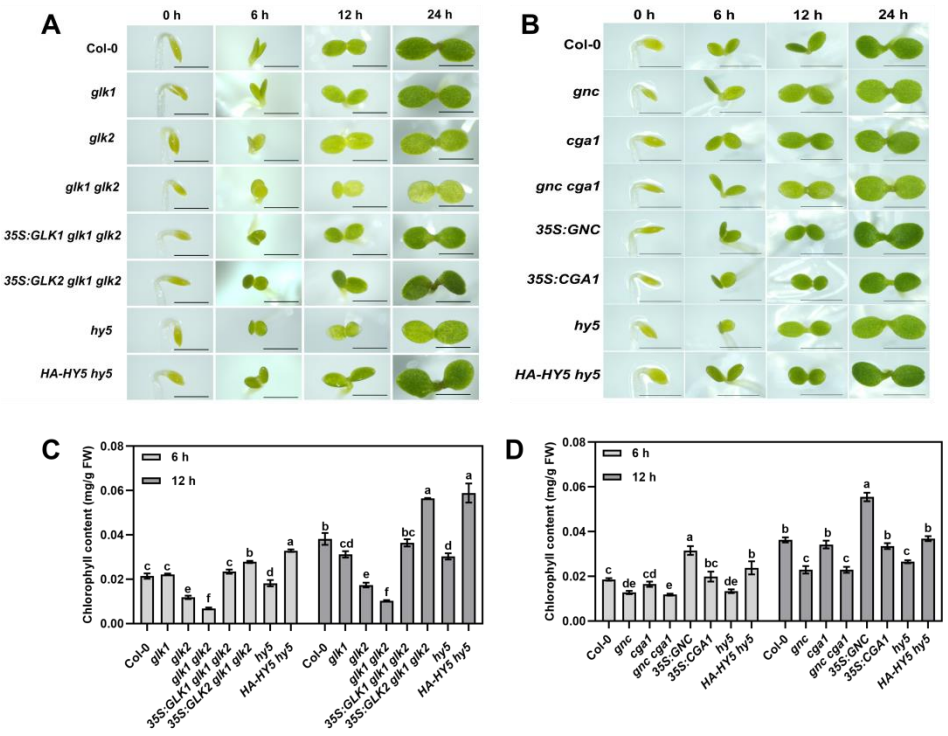

Supplemental Figure S1. HY5, GLK, GNC and CGA1 regulate the chlorophyll content. (Supports Figure 1)

(A) Representative images of 4-day-old etiolated seedlings of Col-0, *glk1*, *glk2*, *glk1 glk2*, *35S:GLK1 glk1 glk2*, *35S:GLK2 glk1 glk2*, *hy5*, and *HA-HY5 hy5* during the transition from dark to light conditions for 6 h, 12 h, and 24 h. Scale bars = 1 mm.

(B) Representative images of 4-day-old etiolated seedlings of Col-0, *gnc*, *cga1*, *gnc cga1*, *35S:GNC*, *35S:CGA1*, *hy5*, and *HA-HY5 hy5* during the transition from dark to light conditions for 6 h, 12 h, and 24 h. Scale bars = 1 mm.

(C) Chlorophyll contents of 4-day-old etiolated seedlings from **(A)** during the transition from dark to light conditions for 6 h and 12 h. The data represent means ± SD (n=3) and letters above the bars indicate significant differences ($P < 0.05$), as determined by one-way ANOVA with Turkey's HSD test. The experiments were performed three times with similar results.

(D) Chlorophyll contents of 4-day-old etiolated seedlings from **(B)** during the transition from dark to light conditions for 6 h and 12 h. The data represent means ± SD (n=3) and letters above the bars indicate significant differences ($P < 0.05$), as determined by one-way ANOVA with Turkey's HSD test. The experiments were performed three times with similar results.

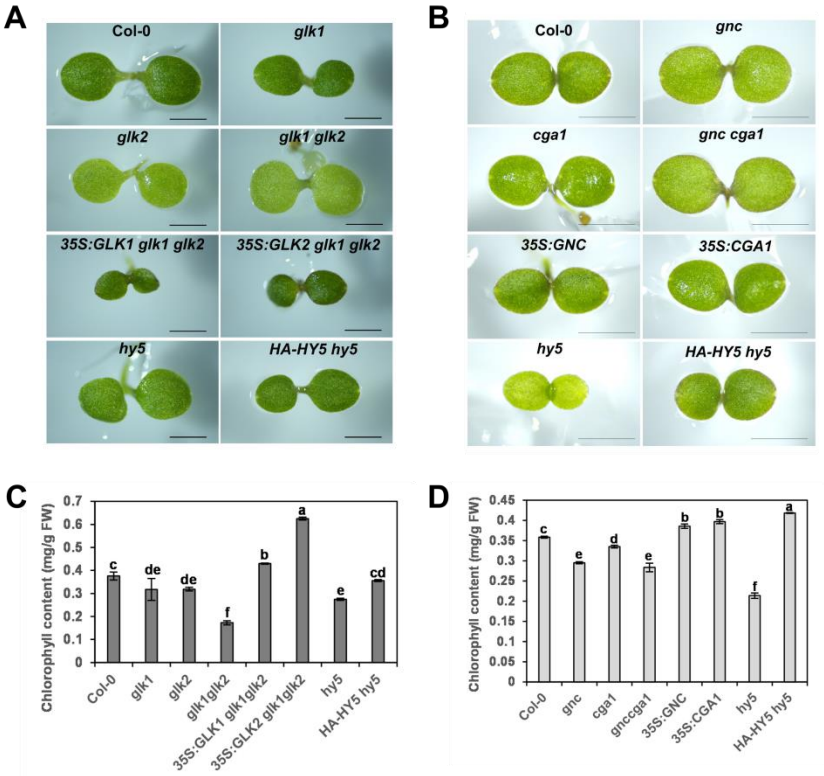

Supplemental Figure S2. Phenotypes of the mutants and overexpression lines under continuous light conditions. (Supports Figure 2)

(A) Representative images of 4-day-old Col-0, *glk1*, *glk2*, *glk1 glk2*, *35S:GLK1 glk1 glk2*, *35S:GLK2 glk1 glk2*, *hy5*, and *HA-HY5 hy5* seedlings grown on half-strength MS plates for 4 days under continuous white light conditions. Scale bars = 1 mm.

(B) Representative images of 4-day-old Col-0, *gnc*, *cga1*, *gnc cga1*, *35S:GNC*, *35S:CGA1*, *hy5*, and *HA-HY5 hy5* seedlings grown on half-strength MS plates for 4 days under continuous white light conditions. Scale bars = 1 mm.

(C) Chlorophyll contents of the genotypes shown in **(A)**. The data represent means ± SD (n=3) and letters above the bars indicate significant differences ($P < 0.05$), as determined by one-way ANOVA with Turkey's HSD test. The experiments were performed three times with similar results.

(D) Chlorophyll contents of the genotypes shown in **(B)**. The data represent means ± SD (n=3) and letters above the bars indicate significant differences ($P < 0.05$), as determined by one-way ANOVA with Turkey's HSD test. The experiments were performed three times with similar results.

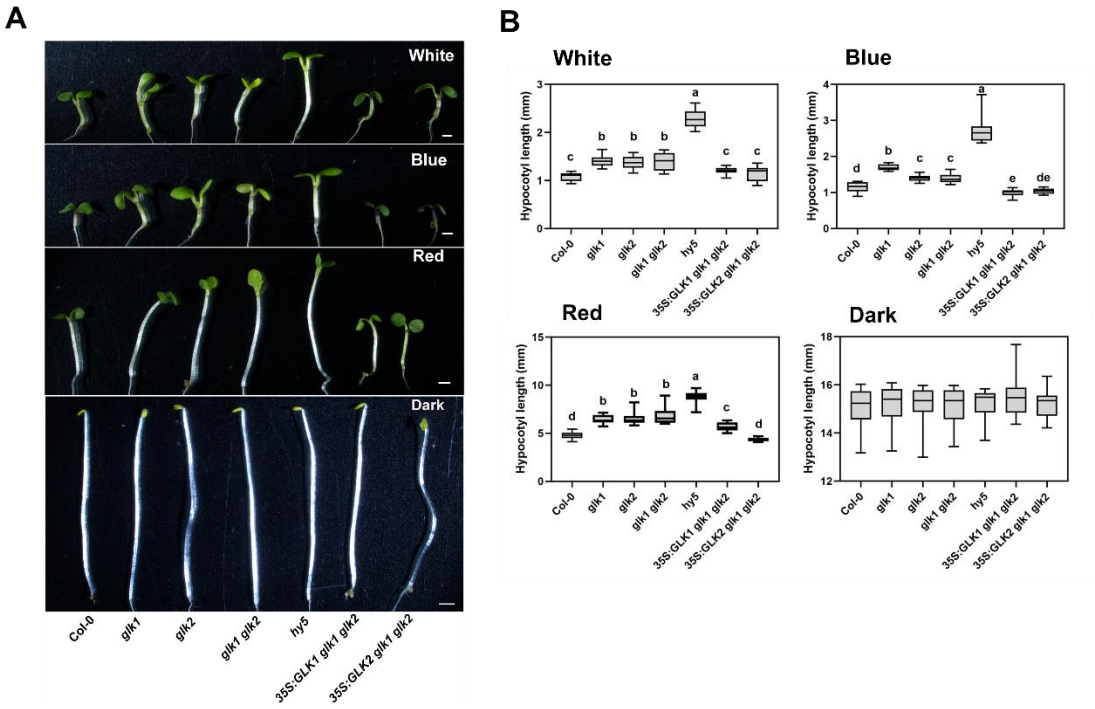

Supplemental Figure S3. GLK inhibits hypocotyl elongation. (Supports Figure 4)

(A) Hypocotyl phenotypes of 4-d-old Col-0, *glk1*, *glk2*, *glk1 glk2*, *hy5*, *35S:GLK1 glk1 glk2*, and *35S:GLK2 glk1 glk2* seedlings grown in white (100 μmol/m^2/s), blue (60 μmol/m^2/s), red (90 μmol/m^2/s) light and dark conditions. Scale bar = 1 mm. **(B)** Quantification of hypocotyl lengths indicated in **(A)**. The data represent means ± SD (n ≥18) and letters above the bars indicate significant differences ($P < 0.05$), as determined by one-way ANOVA with Turkey's HSD test. The experiments were performed three times with similar results.

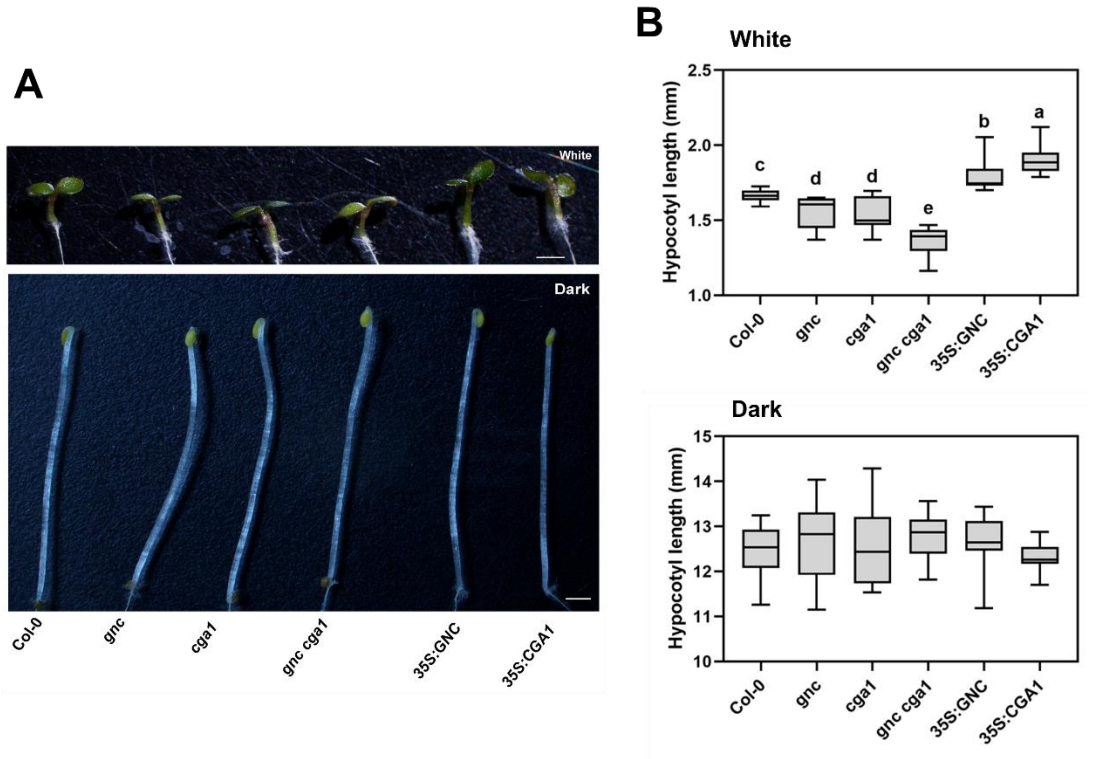

Supplemental Figure S4. GNC and CGA1 promote hypocotyl elongation. (Supports Figure 4)

(A) Hypocotyl phenotypes of 4-d-old Col-0, *gnc*, *cga1*, *gnc cga1*, *35S:GNC*, and *35S:CGA1* seedlings grown in white light (100 μmol/m^2/s) and dark conditions. Scale bar = 1 mm.

(B) Quantification of hypocotyl lengths indicated in **(A)**. The data represent means ± SD (n ≥15) and letters above the bars indicate significant differences ($P < 0.05$), as determined by one-way ANOVA with Turkey's HSD test. The experiments were performed three times with similar results.

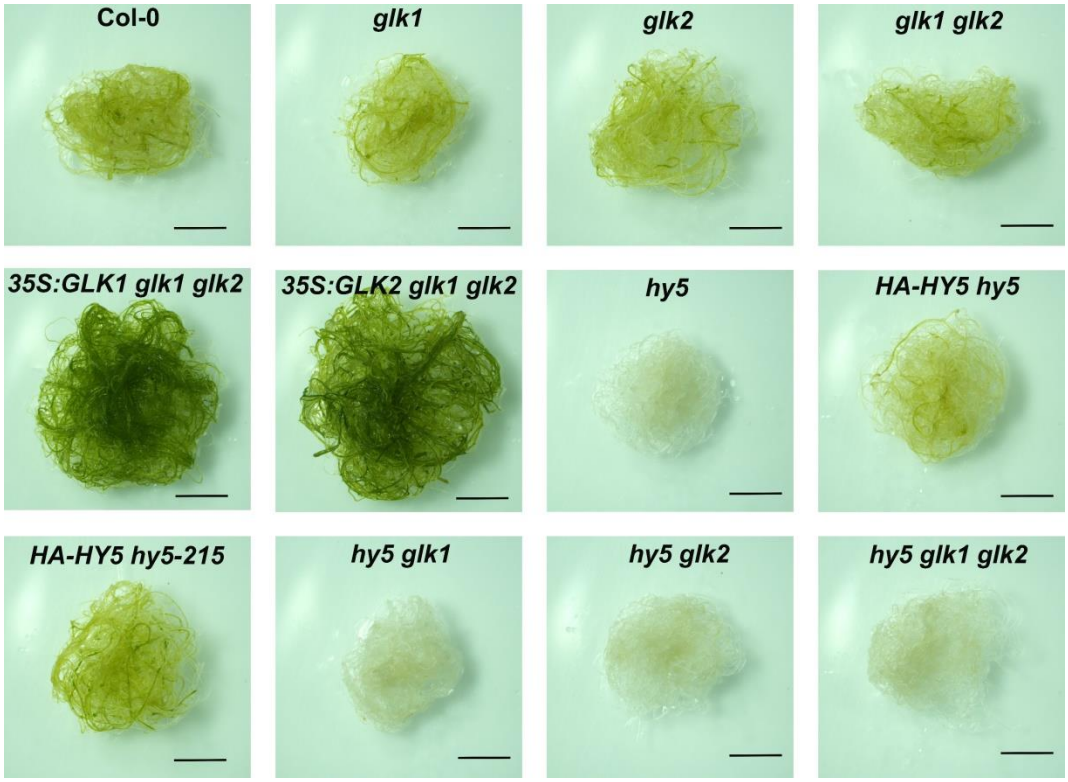

Supplemental Figure S5. HY5 but not GLKs is crucial for the greening of detached roots.

Root samples were detached from 7-d-old seedlings, and then cultured on hormone-free MS medium for 14 d. Scale bar = 5 mm.

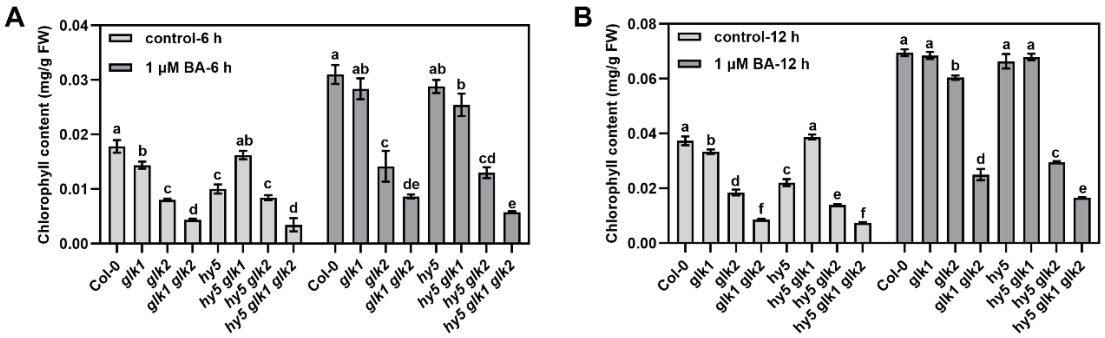

Supplemental Figure S6. 6-BA promotes the GLK and HY5 dependent chlorophyll content.

Chlorophyll content of 4-day-old etiolated seedlings of Col-0, *glk1*, *glk2*, *glk1 glk2*, *hy5*, *hy5 glk1*, *hy5 glk2*, and *hy5 glk1 glk2* grown on medium with or without 6-BA during transition from dark to light conditions for 6 h **(A)** and 12 h **(B)**. The data represent means ± SD (n=3) and letters above the bars indicate significant differences ($P < 0.05$), as determined by one-way ANOVA with Turkey's HSD test. The experiments were performed three times with similar results.

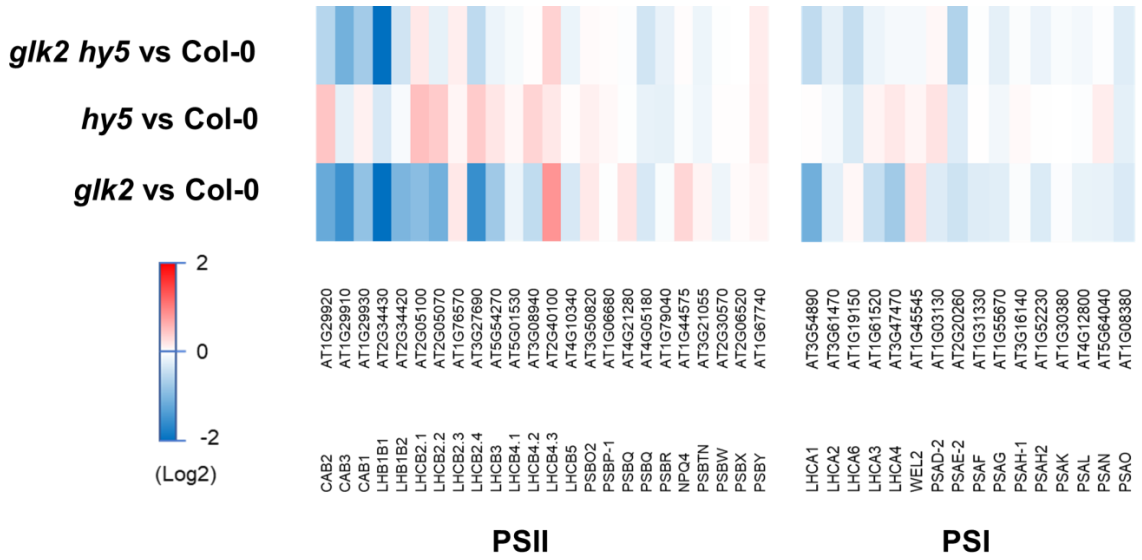

Supplemental Figure S7. Different expression patterns of HY5 and GLK2 regulated photosystem genes.

Expression patterns of Photosystem II and Photosystem I genes in *glk2*, *hy5* and *hy5 glk2* mutants relative to Col-0. The scale bar shows fold changes (log2 value).

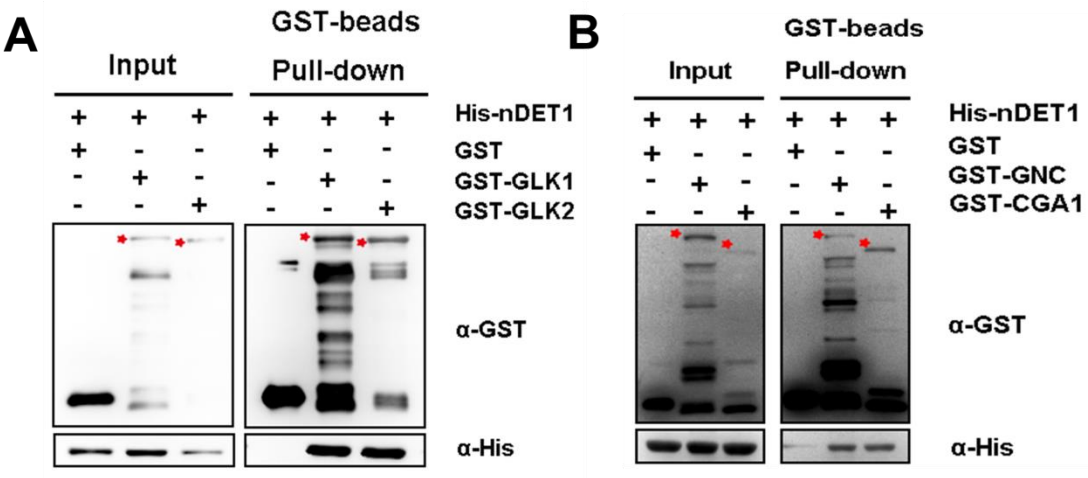

Supplemental Figure S8. *In vitro* evidence of DET1 interacting with GLK and GNC/CGA1 proteins.

In vitro pulldown assays showing the interactions of GLK1, GLK2 (A), GNC and CGA1 (B) with DET1. GST-GLK1, GST-GLK2, GST-GNC, GST-CGA1 or GST proteins were used to pull down His-nDET1 protein using GST beads. Anti-GST and anti-His antibodies were used for immunoblot analysis. “-” and “+” indicate the absence and presence of corresponding proteins.